Transcriptomic profiling of the adult reptilian dentition sheds light on the genes regulating indefinite tooth replacement

Joaquin Ignacio Henriquez[1], Stephane Flibotte[2], Katherine Fu[1], Edward Zirui-Wang Li[1] and Joy M. Richman[1]+

1 - Department of Oral Health Sciences, University of British Columbia, Canada

2 – Bioinformatics Core, Life Sciences Institute, University of British Columbia, Canada

+ corresponding author:
Dr. Joy Richman
2350 Health Sciences Mall
Life Sciences Institute
University of British Columbia
Vancouver, B.C., V6T 1Z3
778-999-8510

Email addresses:

richman@dentistry.ubc.ca
jhenri01@student.ubc.ca
stephane.flibotte@ubc.ca
zirui19@student.ubc.ca
kfu@dentistry.ubc.ca

Key Words: leopard gecko, polyphyodont, successional teeth, gene expression, Semaphorins, odontoclasts, patterning mechanisms

Abstract

The aim of this study is to profile the transcriptomes of teeth and the surrounding tissues of an adult lizard dentition (*Eublepharis macularius*) that is actively replacing teeth throughout life. Bulk RNAseq was used to compare teeth that are in function versus unerupted, developing teeth and single cell RNA-seq was carried out on jaw segments containing the dental forming tissues. In bulk RNAseq data, we found that functional teeth expressed genes involved in bone and tooth resorption. Indeed, multinucleated odontoclasts were abundant in tissue sections of functional teeth undergoing resorption. These are the first steps towards characterizing odontoclasts that participate in physiological resorption. Unexpectedly, chemotaxis gene *SEMA3A* was expressed within odontoblasts and in adjacent mesenchyme, confirmed using RNAscope. Semaphorins may be involved in regulating odontoclasts during tooth resorption. The scRNA-seq experiment successfully isolated dental mesenchyme and epithelial cells. We confirmed that some of these genes are expressed in the earliest tooth buds within the tooth forming field. In addition, we found evidence of convergent evolution in the tooth eruption trait. Geckos evolved a means for second generation teeth to communicate with the functional teeth. Instead of a dental follicle inducing an eruption pathway as in the mammal, the gecko and other squamate reptiles use the enamel organ of the successional teeth to trigger tooth resorption of the functional teeth, thus creating an eruption pathway. New molecules such as SEMA3A may also participate in this process. Future studies on the gecko will uncover the molecular basis of convergent evolution in the dentition.

Introduction

Tooth replacement is the process by which a functional tooth present in the oral cavity is shed and a successor tooth erupts and takes its place. There is a great diversity across species about the number of times that tooth replacement occurs during the life span of an animal ranging from life-long replacement (Polyphyodonty) to no replacement (Monophyodonty). Most non-mammalian vertebrates including fish, amphibians and reptiles are polyphyodont (Tucker and Fraser 2014). In the mammalian lineage the common pattern is for partial diyphyodonty. In humans there are 20 primary teeth that are replaced with the incisors, canines and premolars however molars are added posteriorly from the extension of the dental lamina (Juuri and Balic 2017). Mice and other rodents have a reduced number of teeth including 3 molars that are not replaced and continuously erupting incisors maintained with an active stem cell population in the cervical loops(Yu and Klein 2020). A major gap in knowledge about the dentition is evident since the majority of dental development has been characterized in the mouse model which does not undergo tooth replacement. Another reason for a lack of understanding of tooth replacement is that the actual process of tooth replacement occurs postnatally in humans (Ooë 1981) and all other diphyodont mammals such as pigs (Wang et al. 2014b), ferrets (Jarvinen et al. 2009)and shrews (Järvinen et al. 2008; Yamanaka et al. 2010). Thus far, only the molecular events of permanent tooth budding have been studied during the late fetal period in a small number human fetal specimens (Dong et al. 2014; Wang et al. 2014a) and other mammals (Järvinen et al. 2008; Yamanaka et al. 2010). Animals that replace their teeth more than once are also being used in research studies. The bony fish have replacement of their teeth in an irregular pattern so and some molecular pathways involved in the process have been uncovered (Fraser et al. 2013). Many reptiles replace their teeth (crocodilians, snakes and lizards) throughout life. Previous longitudinal studies on alligators(Edmund 1962) and lizards (Cooper 1966; Grieco and Richman 2018; Kline and Cullum 1984) revealed waves of replacement that appear to be temporally and spatially regulated. Out of all these animals we have selected the leopard gecko, *Eublepharis macularius* for our research because the animals replace their teeth frequently in a highly patterned manner (Brink et al. 2022). Molecular studies have been carried out on the gecko, partially characterizing the main processes of tooth initiation, and differentiation (Brink et al. 2021; Handrigan et al. 2010; Handrigan and Richman 2011; Kim et al. 2020; Zahradnicek et al. 2014).

In the leopard gecko, each functional tooth occupies a position at the margin of the jaws. There are approximately 40 teeth per quadrant of the mouth. Under each functional tooth is a tooth family attached to a long dental lamina. The 2nd generation teeth consist of a mineralizing crown of enamel and dentin surrounding a dental papilla. The 3rd generation teeth are very early in development, either bud stage or early cap stage. The enamel organs of geckos and other reptiles are similar to those in mammals consisting of an inner enamel epithelium that gives rise to ameloblasts, the intermediate stellate reticulum and the outer enamel epithelium. The differences compared to mammals are that in the reptile there is no clear primary enamel knot, the main signaling centre in mammalian cap stage teeth. There is also not a clear stratum intermedium in reptilian enamel organs. The enamel organs are continuous with the dental lamina that connects the 3 generations of teeth together. The dental lamina continues past the 3rd generation tooth to form the successional lamina. The functional teeth eventually are shed by a resorptive process and the next generation tooth erupts to fill the spot. The full tooth cycle from start to finish takes about 4 weeks in the gecko. This means that by harvesting jaw tissues of the adult gecko for RNA profiling we will capture all stages of tooth development.

Only one previous study looked at the molecular basis of tooth shedding in reptiles (Fuenzalida et al. 1999). This study employed Tartarate Acid Resistant Phosphatase staining (TRAP) to identify multinucleated, TRAP+ cells in *Liolaemus gravenhorsti*. These TRAP+ cells were termed odontoclasts since they were located inside the pulp cavities. Similarly, human deciduous teeth have large numbers of TRAP+ odontoclasts that cause rapid resorption of the roots (Sahara 2001; Takada et al. 2004). To move the field forward it is necessary to profile resorbing teeth in a more comprehensive manner. Selecting the leopard gecko allows access to large numbers of teeth participating in physiological tooth resorption. In addition, collection of comparison samples of non-resorbing developing teeth is feasible in the gecko. Both resorbing and developing teeth can be collected in a non-invasive manner (animals can return to the colony). These comparisons between shedding and developing teeth will also highlight developmentally regulated genes that may be novel in terms of a role in tooth formation. Conservation of some but not all genes with mammals is also likely. The reason we expect there to be differences is that geckos and non-crocodylian reptiles lack a periodontal ligament. The periodontal ligament connects the root to the bone in mammals and is derived from the dental follicle. Some snakes appear to have small remnants of Sharpey's fibres that insert into the bone

next to the teeth (LeBlanc et al. 2017; LeBlanc et al. 2021) but these are radically reduced in these animals. There is no evidence of a dental follicle in our analysis of embryonic snakes and lizards to date. Thus it will be interesting to see whether markers of the dental follicle are present in geckos and which cells express these genes.

Finally, the presence of stem cells has been best characterized in the mouse incisor (Chiba et al. 2020; Harada et al. 1999; Krivanek et al. 2020; Sharir et al. 2019). Using elegant lineage tracing and pulse-chase lineage tracing, the dental epithelial stem cells reside in the labial cervical loop (Krivanek et al. 2020; Sharir et al. 2019). We have also searched for putative stem cells in the gecko and found that the dental lamina is a source of stem cells (Brink et al. 2021; Handrigan et al. 2010). Markers for stem cells have only been mapped to a very limited extent in the gecko (Handrigan et al. 2010). It is necessary to move towards single cell RNAseq and to enrich for epithelium to find more genes that identify rare populations of progenitor/stem cells. A previous study on bearded dragon used laser capture microdissection of the successional lamina to identify differences that are present in cells that will form successional teeth versus those that do not participate in tooth succession. There were very few gene differences identified so a more comprehensive method is required with less disruption of the cells.

In this paper we used a combination of bulk and single cell, next generation sequencing technology followed by validation with several methods. We report genes that were not previously associated with tooth development, tooth replacement or tooth resorption. In addition markers of specific areas of mammalian teeth are found in gecko teeth, even though the homologous structures are not present. These unbiased studies will set the stage for future tests of the role of chemotaxis and epithelial-mesenchymal interactions take place under physiological conditions in the adult jaw.

RESULTS

Our aim was to take an unbiased approach to examine the differences in expression in functional teeth versus developing teeth. We predicted that the main processes that characterize developing teeth would include genes involved in odontogenesis, pulp cell maintenance and genes required to stimulate clastic cells differentiation. The scRNA-seq data was carried out with a different intent. Here we wanted to uncover cell populations that were recognizably dental but also expressed genes not have previously been noted as a part of tooth development. We also wanted to overcome the barriers of using a non-model organism, the leopard gecko in a full, unbiased transcriptome analysis.

Quality control of samples used for bulk RNAseq

We first performed a principal component analysis of the samples using the count matrix from STAR method (Fig S1). Principal component (PC) 1 explained 40.6% of the variability of the data, PC2 explained 22.47%. The functional tooth samples grouped together in the negative quadrants of PC1 axis while developing tooth samples grouped in the positives quadrants (Fig. S1A). Interestingly, PC2 accounted for the differences between animals (Fig. S1A). The samples belonging to animal 1 (two developing and 1 functional sample) were on the positive side of PC2 axis. The negative region of PC2 contained samples belonging to animal 2. Hierarchical clustering computed from the STAR matrix showed similarity within the functional tooth samples and within the developing samples (Fig. S1C).

A total of 16,954 genes were sequenced across the samples. We performed a 5 pipeline analysis as described in Vuilleumier et al (Vuilleumier et al. 2019) to align and count the reads for each sample, generating 5 matrices. Two differential gene expression analysis were performed using edgeR and DESeq2 for each one of the matrices. The reported p-value and $\log_2$ fold change were calculated by averaging the result of applying edgeR to each of the five matrix (Fig. 2A). The same applies for the DESeq2 (Fig S2A). A total 1,139 transcripts were significantly differentially regulated in any of the two differential gene expression analyses (Table S1). Of these, 264 genes were downregulated and 875 were upregulated in developing teeth. Of the total downregulated and upregulated genes, 190 and 567 have an FDR lower than 0.05 in edgeR and DESeq2, respectively (Table S1). This list of significantly regulated genes

was further annotated using the NCBI tool blastx and the non-redundant data base due to the high number of transcripts labelled as “unknown” or other codes that are not gene IDs. We started with 34% of genes (390/1139) that fell into this category. After the blastx annotation the list of unknown genes decreased to 19% (212/1139). These efforts were necessary in order to perform post-hoc analyses such as Gene Ontology to identify enrichment for certain biological processes.

Transcripts upregulated in developing teeth.

Developing teeth collected during the microdissections are primarily in bell stage since we rely on calcein incorporation and this dye is only incorporated once mineralization has taken place (bell stage). As expected genes required for early ameloblast differentiation were enriched in developing teeth. Ameloblastin (AMBN) is second most abundant proline-rich matrix glycoprotein in enamel(Moradian-Oldak and George 2021). *AMBN* was significantly upregulated in developing teeth (Fig. 2A; $\log_2 = 4.66$; Fig. 2B, 5-fold enriched). Amelotin (AMTN; $\log_2 = 3.95$) and MMP20 are also part of enamel synthesis and are upregulated in developing teeth (Bartlett and Simmer 2015; Hu and Simmer 2007).

In the present study the bulk dissection of bell stage teeth captured inner enamel epithelial transcripts. In the mammal, *Shh* (Sonic Hedgehog) is expressed in the primary enamel knot and inner enamel epithelium in placode, bud, cap and bell stage mouse teeth (Vaahtokari et al. 1996). We have also published expression of *SHH* in gecko teeth, particularly in the inner enamel epithelium of bell stage teeth, prior to differentiation of the ameloblasts (Handrigan and Richman 2010). *SHH* was more highly expressed in developing teeth (Fig. 2A; $\log_2 = 6.19$) and this was validated with qRT-PCR (Fig. 2B; 18-fold higher than functional teeth). Target genes of the Hh pathway are also upregulated in developing teeth including *PTCH1* ($\text{Log}_2 = 3.8$) and *GLI1* ($\text{Log}_2 = 3.36$). Another dental epithelial gene, *EDAR* (Ectodysplasin receptor, $\log_2 = 2.09$; Table S1) is also more highly expressed in developing teeth. In the mouse, *Edar* is exclusively expressed in the dental epithelium at placode, bud and cap stages(Laurikkala et al. 2001). *Edar* is also strongly expressed in the primary enamel knot of (Laurikkala et al. 2001) however gecko teeth do not appear to have a primary enamel knot (Handrigan and Richman 2011). Thus the function of EDAR in the replacing reptile dentition may be different than in mammals. *TSPEAR* (Thrombospondin type laminin G domain and EAR repeats) was also upregulated in developing

teeth (log_2 =2.59) (Table S1). Mutations in human *TSPEAR* produce ectodermal dysplasia type 14 (OMIM: 618180) which also is characterized by hypodontia (Peled et al. 2016).

We identified several genes that are expressed more highly in the dental mesenchyme (Fig. 2A; log_2 1.82; Fig. 2B; 2.8 fold). *LHX8* is a transcription factor that is expressed in early neural-crest derived mesenchyme and in dental mesenchyme of developing mouse molars (Grigoriou et al. 1998; Zhao et al. 1999; Zhou et al. 2015). Follistatin is highly expressed in dental mesenchyme in mouse teeth (Wang et al. 2004) and is also increased in developing gecko teeth (Log_2 = 7.33). *Fgf3* is highly expressed in the early odontoblast layer of mouse molars (Popa et al. 2019) and is upregulated in the developing gecko teeth (Log_2 = 5.22) Interestingly, *Sfrp2* (Secreted Frizzled Related Protein 2) a WNT (Wingless-related protein) antagonist, is expressed in the dental follicle in the mouse dentition Fig. 2A, log_2 = 1.41) (Table S1)(Sarkar and Sharpe 1999). Since the gecko does not form a dental follicle, the gecko *SFRP2* transcripts must be in a different cell type. The location of *EDAR*, *TSPEAR* and *SFRP2* transcripts or proteins and many others will need to be mapped in the gecko dentition. Overall, the expression of genes in developing gecko teeth contains genes found in the embryonic mouse molar but there is a subset of genes such as *EDAR* and *SFRP2* that may have radically different spatial locations of transcripts compared to the mammal.

Transcripts upregulated in functional teeth

We were also interested in identifying genes relevant to tooth homeostasis by profiling expression in functional teeth. *SPARC* (Secreted acidic cysteine rich glycoprotein or Osteonectin) which has an important role in biomineralization of bone was more highly expressed in functional teeth (log_2 = -1.4) (Fig. 2A, B). *SPARC* and mutations in this gene in human cause osteogenesis imperfecta type XVII (OMIM# 616507). Thus far, tooth phenotypes have not been associated with mutations of the *SPARC* gene (Mendoza-Londono et al. 2015). In addition, we identified two novel genes, not previously known to be involved in tooth function including *ELF3* (log_2 = -2.43; Fig. 2A,B) and *NT5E* (log_2 = -2.43; Fig. 2A,B). *Elf3* (E74-like factor 3), is expressed in salivary gland(Song et al. 2022), hair follicle(Choi et al. 2008) and mammary gland (Choi et al. 2009). Since all of these are ectodermal derivatives, it is possible that expression of *ELF3* in functional gecko teeth is in the only areas with residual epithelium, the cervical loops. There are no mouse studies that examined expression of *Elf3* in the dentition.

NT5E is a nucleotidase that when mutated causes ectopic calcification of joints and arteries (OMIM: 211800) (St Hilaire et al. 2011). Again *Nt5e* has not been mapped in the mouse dentition. We also identified significantly enriched transcripts for *GPRC5A* in functional teeth (G protein-coupled receptor, family C, group 5, member A ($\log_2$ = -3.74; Fig. 2A). *GPRC5A* is a 7-transmembrane G protein coupled receptor, whose expression is induced by retinoic acid (Cheng and Lotan 1998). The ligand for GPRC5A has not been identified (Richter et al. 2020) and there is no known role for this gene in odontogenesis.

Bulk RNAseq identifies genes associated with root resorption in functional teeth

Interestingly, genes expressed by osteoclasts such as *ACP5* and *CSF1R* (Fig. S2A, 2B), were upregulated in functional teeth. In addition, *PTHLH,* a potent inducer of RANKL (Rao et al. 2018) a classic osteoclast differentiation factor, was upregulated in developing teeth (Fig. 2A, B). The macrophage marker *CD-68* ($\log_2$ = -1.34) is also upregulated in functional teeth (Fig 2A, S2B). *CD68* is expressed in fully differentiated osteoclasts and not their precursors (Jackson et al. 2017). *TGFβ*-1 was at the edge of the significant genes described by edgeR analysis (Fig. 2A; $\log_2$ = -1.17). In qRT-PCR we found significantly elevated expression of *TGFB1* in functional teeth (Fig. S2B). *TGFB1* signals via the transcription factor Smad4 and there is evidence that TGFB1 protein activates ostoclastogenesis in mice (Morita et al. 2016). The location of all of the aforementioned gene transcripts and their role in the adult gecko tooth has not been explored.

We next examined the functional teeth in detail to see whether there were odontoclasts within the pulp cavity. The odontoclast is similar to an osteoclast but has not been as well characterized (Wang and McCauley 2011). A microscopic analysis of the functional teeth showed the presence of many multinucleated cells inside resorption pits (Fig. 3A,A'; Fig. S6C) but an absence of multinucleated cells in developing teeth (Fig. 3A''). Not all functional teeth are shed at the same time (Grieco and Richman 2018) so we expected approximately every other tooth to be invaded by odontoclasts. Indeed using the TRAP stain (Tartrate resistant acid phosphatase is coded by the *ACP5* gene) a marker for odontoclasts (Fuenzalida et al. 1999; Lee et al. 2020; Sahara et al. 1996; Takada et al. 2004), showed many TRAP+ cells inside the pulp cavities of resorbing teeth (Fig. 3B,B'; Fig. S6D,F,H) but not in developing teeth (Fig. 3B''). Interestingly, the egg tooth found only at hatching also contains TRAP+ cells that are involved in shedding of the tooth (Fig. S6A,B). TRAP staining indicates that odontoclasts are actively

resorbing dentin, however there are other markers that identify earlier stages of odontoclast formation. We used antibodies that recognize RANKL (Rank Ligand) and CTSK (Cathepsin K). The multinucleated cells that stained with TRAP were also positive for CTSK and RANKL (Fig. 3C'-E'). Developing teeth did not have positive cells in the pulp cavities (Fig. 3C''-E''). However, on the labial side of developing teeth (near the bone) there were small groups of TRAP+ and CTSK+ cells that were negative for RANKL (Fig. 3B''-E''). These cells are also mononuclear and therefore could be precursor monocytes that are migrating towards the pulps of functional teeth.

The robust expression of the CTSK antibody prompted us to search the RNAseq data for the transcripts. Surprisingly, there were no *CTSK* transcripts in the data. Neither could we identify a coding sequence for *CTSK* in the draft *E. macularius* genome (Xiong et al. 2016) even by blasting with the *Gekko japonicus CTSK* sequence. Next we took individual exons *G. japonicus* and aligned these to the *E. macularius* genome. After predicting exon-intron boundaries in the *E. macularius* scaffolds (Table S2), we successfully identified the orthologue of *CTSK*. We performed the transcriptome analysis again and found significantly elevated *CTSK* in gecko functional teeth (Fig S2D). This one gene exemplifies some of the issues with the draft *E. macularius* genome. The shotgun reads were very short and exon-intron boundaries could not be identified accurately. From our estimates, about 40% of genes were not correctly annotated.

An unexpected class of genes that was expressed in gecko functional and developing teeth belonged to a class of chemotaxis molecules, the Semaphorins. *SEMA3A* and *SEMA3E* are primarily known as guidance molecules for the nervous system and angiogenesis. *SEMA3E* was downregulated in developing teeth when compared to functional teeth, whereas *SEMA3A* had the opposite trend (Fig. 2A). *SEMA3E* differential expression was significant in both edgeR and DESeq2, while *SEMA3A* was significant only in DESeq2. SEMA3A has been shown to be a chemo repellant that controls timing of tooth innervation in the mouse (Luukko and Kettunen 2016; Moe et al. 2012a; Moe et al. 2012b; Shrestha et al. 2014). SEMA3E is best known in regulating vascular patterning in mammals and not odontogenesis (Kim et al. 2011). Moreover, there does not appear to be *Sema3e* expressed in developing mouse teeth (Fu et al. 2017).

Unlike in the mouse, we localized transcripts for both *SEMA3A* and *3E* in the gecko dentition using RNAscope (Fig. 4A-D'). *SEMA3E* was expressed in the odontoblasts and in

mesenchyme external to the tooth root (Fig. 4A-A''). In developing teeth, *SEMA3E* was in the odontoblast layer (Fig. 4B,B'). *SEMA3A* was expressed in the differentiated odontoblasts of functional teeth and external to the teeth (Fig. 4C'C''). In developing teeth, *SEMA3A* was mostly expressed in the apical papilla in between the cervical loops, a pattern not seen with *SEMA3E* (Fig. 4D,D'). There was also expression of *SEMA3A* external to the developing tooth (Fig. 4D'). It is interesting that *SEMA3A* acts as a chemorepellant for nerves in the murine dentition (Luukko and Kettunen 2016). We suspect that the strong apical presence of *SEMA3A* delays nerve ingrowth until the tooth is more fully developed. There may also be novel functions of SEMA3A in the regulation of odontoclasts.

Single cell RNAseq identifies clusters of dental epithelial and mesenchymal cells

The reasons for carrying out bulk RNAseq specifically on the dissected teeth were that we could be sure that all genes identified would be specific to the teeth and not surrounding tissues. The comparison between bell stage and functional teeth was designed to identify genes required for tooth shedding, eruption and those needed for crown completion. Other cells adjacent to the developing teeth, particularly the dental lamina and successional lamina are critical for tooth initiation in the adult gecko (Brink et al. 2021). We turned to single cell RNAseq in order to isolate cells comprising the tooth field deep in the jaws. This dissection included dental lamina, successional lamina, early tooth buds, bell stage teeth, oral connective tissue and mucosa. We obtained 6,197 cells, 68,380 post normalization mean reads per cells and 492 median genes per cell (Fig. S5).

We carried out two different cell isolation protocols in order to see whether yield was better at cold temperatures as had been reported (Adam et al. 2017)(Fig. 1B). The body temperature of the gecko is 28-32°C so it was necessary to try a different method that may be more compatible with ectothermic animals. The quantity of genes per cell was higher (Fig. S5A,C) and the number of molecules per cell was higher at colder temperatures (Fig. S5B). Using the Cell Ranger pipeline, the number of genes per cells and unique molecular IDs or bar codes were also higher in the *B. lichenoformis* method (Fig. S5C).

Next, we began by looking for patterns of cells isolated with the two different isolation methods from two different animals (Fig. 5B). Using the Seurat package in R, we computed 12 clusters and a list of differentially expressed transcripts (Table S3). We used FindClusters

(resolution = 0.2). All cells were included with nFeature or gene IDs between 175 and 2600. As with the bulk RNAseq we used the Blastx function to identify the human orthologous gene name for the 45% unknown genes (662 genes/1458 unknown genes). After performing Blastx, the number of non-useful annotations decreased to 21% (307/1458). A gene ontology analysis was carried out using GO Consortium and we used the Biological processes (Table S4) to assign identities to 6 out of 12 clusters, 2 with certain dental identity (cluster 3 and 6) and one with a mix of dental and non-dental cell types (0). There were other clusters containing non-dental cell types (1,5,9).

Most of the clusters were comprised of a mix of cells isolated with the cold and warm enzyme treatments, however cells in clusters 1,2,3,5,7,8 and 9 came almost exclusively from the animal (maxilla) dissociated with collagenase/dispase (Fig. S6). Clusters 4,6,10 and 11 came mainly from the cold temperature isolation (animal 2, mandible). Cluster 0 also had 40% of the cells come from the cold technique. Thus both methods have advantages and disadvantages and combining the two types of isolation methods helps to ensure populations of cells are not missed. It is more likely that the type of enzyme was responsible for the differences in cells that were isolated rather than the animal or the region of the jaw. We have seen interchangeable results in the maxillary or mandibular teeth in previous work (Brink et al. 2021) and data not shown.

Cluster 0 was confirmed as epithelial since multiple keratin transcripts were present (Table S3, Fig. 5C; Fig S8B-F; *KRT 4, 5, 12, 14, 23, 24*). In humans, keratin 5 (a type I keratin) and 14 (a type II keratin) form a pair that is expressed in the keratinocytes of the basal layer of the epidermis, the basal cells of endodermally-derived glands and other stratified epithelia (Porter and Lane 2003). Mutations in *KRT5* or *KRT14* produce epidermolysis bullosa simplex (Porter and Lane 2003). Antibodies to KRT14 strongly stained cells of the human dental lamina (Domingues et al. 2000). Cluster 0 also contains cells that express a known dental identity gene, *PITX2* (Fig. 5C)(Thesleff 2014) and *SOX2* a, dental epithelial stem cell marker (Fig. S8K)(Yu and Klein 2020). Mutations in *PITX2* cause Axenfeld Rieger syndrome type I (OMIM: #180500), which also features dental anomalies. The gap junction gene, *GJA1* (codes for Connexin 43) is also expressed in the epithelial cluster 0 (Fig. 5C). Mutations in *GJA1* cause oculo-dento-digital dysplasia syndrome (OMIM: #164200). Therefore, cluster 0 consists of dental and non-dental epithelial cells.

Cluster 6 had a higher proportion of dental epithelial gene transcripts (Table S3; Fig. 5F; Fig. 6A). Cluster 6 expressed *PITX2*, which is strongly expressed in the enamel organ of developing teeth and successional lamina (Fig. 6A,B). We previously mapped in detail the expression of PITX2 in the leopard gecko dentition (Brink et al. 2021). *GJA1* which codes for Connexin43 is also expressed strongly in cluster 6 (Fig. 6A). CX43 protein mainly restricted to the enamel organ of developing teeth (Fig. 6C) but absent in the dental and successional laminae. Ameloblasts in the inner enamel epithelium at secretory stages have intense signal particularly in the lateral aspect of the cell membranes (Fig. 6C, S7B-B'') as described in the mouse (Toth et al. 2010). Mice with a heterozygous loss-of-function mutation in *Gja1* have poor quality, thin enamel (Toth et al. 2010). We verified that CX43 protein is present at lower levels in the odontoblasts and dental papilla (Fig. 6C', S7B'). Thus, in the gecko, CX43 was not exclusively expressed in epithelial cells, as reported in the mouse (Toth et al. 2010). Cells in cluster 6 express other genes found in the enamel organ including *SHH* (Table S3). *SHH* was previously shown to be expressed in the embryonic leopard gecko enamel organ (Handrigan and Richman 2010). Cluster 6 cells expressed *Fermt1* (Rostampour et al. 2019), *Irx1*(Yu et al. 2017), *Ednrb* (Neuhaus and Byers 2007) and *Itgb4* (Salmivirta et al. 1996) all of which are expressed in the mouse enamel organ. Markers of fully functional ameloblasts were not identified in cluster 6, even though these genes were found in the bulk-RNA-seq data for developing teeth. The reason may lie in the difference in dissection methods used for for scRNA-seq. In this enzyme protocol we did not use calcein labeling to identify mineralizing teeth. All such teeth would have been filtered out during the cell isolation process.

Of all the cell groups, Cluster 3 most closely resembled dental mesenchyme (Fig. 5D,E). As predicted by the immunostaining, we did find expression of *GJA1* in cluster 3 cells (Fig. 5D). Markers such as *LHX8, TWIST1*, *TGFB1*, *ALX1* and *OSR2* (Fig 5DE, Fig S9J-L) were highly differentially expressed compared to other clusters (Meng et al. 2015; Zhou et al. 2015). TWIST1 protein is expressed strongly in mesenchyme and in particular in dental mesenchyme of the mouse (Higashihori et al. 2017). In the bearded dragon, *ALX1* was expressed in the dental lamina/successional lamina rather than the mesenchyme (Salomies et al. 2019). *Lhx8* (formerly known as *Lhx7*) is strongly expressed in craniofacial mesenchyme including the tooth bud mesenchyme (Grigoriou et al. 1998) as well as in t the root mesenchyme The *Osr2* transcription factor is express in the mesenchyme lingual to the dental lamina in both the maxilla and

mandible of mice at 11.5. Deletion of *Osr2* in the mouse causes molar duplication (Zhang et al. 2009). Cluster 3 also expressed *COL1A1* (Fig 7A) which is widely expressed in all connective tissues and in the dental papilla of developing teeth (Fig. 7B,C,C'). There is no expression of *COL1A1* in the epithelium (Fig. 7D).

Unidentified genes hinder cluster identity assignment

The remaining clusters had small numbers of differentially expressed genes and using the GO biological process enrichment, identities were not assigned (Table S3; Fig. S11D-O). We identified cluster 1 as most likely being composed of T-cells (Fig. S9B-F, M,N). Key markers of T-cells include *TESPA1* 1, which is involved in T-cell development (Wang et al. 2012). In addition, the HLA group is mainly restricted to cluster 1 (Fig. S9F). Cluster 2 is most likely composed of lymphocytes and other white blood cells (Fig. S9G-I). In cluster 4 we identified enrichment of *TMEM249* and *C3* (Fig. S9M,N) a gene coding for complement which is in the innate immunity cascade). Cluster 5 contained proliferative cells of unknown identity (Fig. S10B,C). The cell express *PCNA, CDK1* (Gautier et al. 1988) and the PCNA associated factor *PCLAF* (Emanuele et al. 2011). Clusters 7 and 8 contain cells secreting cytokines and complement factors (Fig. S10G-I) but the exact cell type is unclear. Cluster 9 expressed genes associated with angiogenesis (Fig S10J-L) like *ROBO4* which is highly expressed in endothelial cells (Jones et al. 2008). Cluster 10 (Fig. S10M-O) and cluster 11 (Fig. S11B-D) have no clear identity.

***PTHLH*, a gene required for tooth eruption, is expressed in bulk and scRNAseq**

PTHLH (Parathyroid hormone-like hormone), was upregulated in the developing teeth in bulk RNAseq (Fig. 2A, B) and was also statistically significantly enriched in the dental epithelial cells of cluster 6 (Fig. 6A, Table S3). *PTHLH* is of biological relevance because of the roles that it plays in tooth development and eruption in mice and human. Mouse *Pthlh* is expressed in the outer enamel epithelium and stellate reticulum while the receptor, *Pth1r*, was mainly expressed in the bone, dental mesenchyme of the pulp and the dental follicle (Philbrick et al. 1998). The same group reported the expression of *Pthlh* in the dental follicle of 8 day postnatal rats (Nakchbandi et al. 2000) so there are conflicting data concerning the epithelial expression of *Pthlh*. Others have shown using lineage tracing that there are Pthlh-expressing cells in the mouse dental follicle which gives rise to the periodontal ligament. (Ono et al. 2016; Takahashi et al.

2019). In addition, lineage tracing for Pth1r confirmed expression in dental mesenchymal derivatives including odontoblasts and dental follicle cells, but not in dental epithelial cells (Takahashi et al. 2019). These authors concluded that the main signaling is taking place in an autocrine manner within the dental follicle. In humans, loss-of-function mutations in *PTH1R*, are associated with primary failure of tooth eruption (Nagata et al. 2020). Knock-out of *Pthlh* in mice prevented tooth eruption (Philbrick et al. 1998). Knock out of *Pth1r* specifically in dental follicle cells also recapitulates human primary failure of eruption (Takahashi et al. 2019). We mapped expression of gecko *PTHLH* with in situ hybridization. Similar to the original mouse data, we found that gecko *PTHLH* was expressed in the cells of the inner enamel epithelium (Fig. 6E,G), stellate reticulum and successional lamina (Fig. 6F,G and Fig. S7A-A''). There were a few transcripts present in the dental papilla (Fig. 6E). The most abundant expression of *PTHLH* was in the second generation teeth, next in line to erupt into the mouth (Fig. S7A''). Therefore, the expression of *PTHLH* in the gecko is more similar to what Philbrick et al. reported for the mouse (Philbrick et al. 1998). The expression of PITX2, GJA1 proteins and *PTHLH* in the same cells strengthens the idea that the enamel organ is the cell type that most highly expresses *PTHLH*. The position of these *PTHLH* transcripts may function in odontoclast recruitment and activation in the functional tooth.

DISCUSSION

In this study we used unbiased transcriptome profiling of the healthy adult reptile dentition that is in the midst of physiological tooth replacement. All stages of the tooth replacement cycle were captured because we used two complementary methods of RNA collection. The bulk RNA-seq included functional teeth that participate in the normal ingestion of food. We also included functional teeth at the end of the life cycle. These teeth no longer have a functioning pulp and instead are invaded by odontoclasts. The odontoclasts rapidly resorb the dentin and the bone-dentin interface allowing teeth to be shed. The other half of the tooth replacement cycle was captured with single cell dissociation of the soft tissues in the jaws. The deepest, most aboral region always contains the nascent tooth forming field. By dissecting jaw regions across several tooth families, we included a range of tooth initiation stages from the successional lamina, tooth bud, cap and bell stage. The dental lamina which is continuous around the jaw was also dissociated and included in the sample. Indeed, using two different enzymatic treatments, helped to improve the yield of cells in the dental epithelial and dental mesenchyme clusters. The data has revealed both conservation and novel aspects of odontogenesis not present in the mouse model.

Cold versus warm isolation methods in scRNA-seq preferentially enrich for different cell types

The novel approach of using scRNA-seq on a reptile motivated us to test two different methods of cell isolation. We used a warm method that requires 37° C temperatures even though this is above body temperature of lizards and most ectothermic reptiles (28-29°C). Thus far we are the only group to use *B. lichenoformis* for dental cell isolation studies. The scRNA-seq studies carried out in mouse teeth use a range of enzymes, usually collagenases, that vary according to research group. The Ono group prefers Liberase (Sigma Aldrich) which is a combination of Collagenase I and II and Thermolysin (Nagata et al. 2021; Ono et al. 2016; Takahashi et al. 2019). The Klein group uses Collagenase II (Sharir et al. 2019). The Chai group uses Collagenase I (Jing et al. 2022), the Krivanek group used Collagenase P, or Collagenase D plus Dispase (Krivanek et al. 2020). The Mitsiadis group used Collagenase P for human teeth (Pagella et al. 2021). We found that there were groups of cells that were preferentially included or excluded depending on the enzyme conditions. In particular, the dental mesenchyme cluster was almost entirely isolated using the warm Collagenase D/Dispase II mixture. Almost all T-

lymphocytes were excluded by *B. lichenoformis* protease which could be a useful way to reduce the number of white blood cells in the isolation procedures. We used the same labeling system as the mouse studies (10X Genomics) and the same type of sequencer. Nevertheless, the quality of data from the gecko scRNA-seq was lower than the mouse particularly when the warmer temperatures were used. Therefore, the cold method is a very useful adjunct and could be used to supplement the more common protease methods used in mouse or human studies.

We were expecting to find groups of progenitor cells in the scRNA-seq data however due to their low numbers these cells were not encountered. It is possible that some of the dental epithelial and mesenchymal cells contained these putative stem cells. Our previous in situ hybridization experiments on adult geckos located expression of stem cell marker *IGFBP5* primarily in the dental mesenchyme (Handrigan et al. 2010). In agreement, we found *IGFBP5* in a subset of dental mesenchyme cells. The other markers we had studied included WNT pathway transcription factors *TCF3* and *TCF4* both of which were expressed mainly in the dental epithelium. *LGR5* was minimally expressed in the dental epithelium as was *DKK3*. None of these genes were identified in the present data. Further validation of gene expression patterns using in situ hybridization or immunostaining is needed to increase our understanding of the adult gecko stem cells that contribute to new tooth formation.

Mouse dental follicle gene signatures are present in gecko

In squamate reptiles (snakes and lizards), the dentin of the root directly fuses to the alveolar bone (bone of attachment) (Bertin et al. 2018; LeBlanc et al. 2021). The leopard gecko has fusion of dentin (contains tubules) to the alveolar bone (woven bone with embedded osteocytes). There is no evidence from our studies (Brink et al. 2021; Brink et al. 2020; Buchtová et al. 2007; Handrigan et al. 2010; Handrigan and Richman 2010; 2011) and those of others (Buchtova et al. 2013; Vonk et al. 2008; Zahradnicek et al. 2014) on prehatching snakes and lizards of a follicle in surrounding the developing teeth. In contrast, the mammals and crocodilians form a thecodont tooth attachment which consists of tooth inside a socket that is connected to the bone via a non-calcified periodontal ligament. The periodontal ligament fibres inserts into the cementum and bone (Bertin et al. 2018; LeBlanc et al. 2021). The origins of the periodontal ligament are mainly from the neural crest-derived dental follicle as shown with lineage tracing experiments (Jing et al. 2022; Nagata et al. 2021; Takahashi et al. 2019). Extensive transcriptome profiling has been carried out on the mouse dental follicle in embryonic

and postnatal stages (Jing et al. 2022; Takahashi et al. 2019). Upon comparing the mouse data to the gecko we were interested to find several cell types that express genes characteristic of the dental follicle. The dental mesenchyme cluster 3 expressed *SFRP2, IGFBP5, FOS* and *SGK1*, all of which are beautifully restricted to the mouse dental follicle. This suggests that there are some mesenchymal cells in the gecko that may not be as well organized as in the mouse but could still take on some roles of the dental follicle. There are several key dental follicle genes not represented in the gecko scRNA-seq data, particularly *Postn, Bmp3* and *Acta2* (Jing et al. 2022). The absence of these key genes is consistent that a periodontal ligament is not formed in the gecko.

Genes required for tooth eruption identified in the gecko bulk RNA-seq data

Currently we know little about how gecko teeth erupt other than some of the key steps are different than in a mammal. Tooth eruption is a functional requirement of the dentition across the entire animal kingdom. The mammal absolutely requires the dental follicle for tooth eruption as shown in studies where an inanimate tooth erupted as long as the follicle was preserved (Cahill and Marks 1980). In rodent teeth, the best characterized system, teeth erupt by first creating an eruption pathway through the bone. Osteoclasts under the control of TNFSF11 (RANK ligand or RANKL) and CSF1 are attracted by the dental follicle above the crown of the tooth. The osteoclasts create an eruption pathway allowing the immature tooth to relocate closer to the oral cavity (Wise 2009; Wise and King 2008). The pre-eruptive phase of tooth eruption also requires activity of the PTH pathway mediated by the interaction of PTHLH and the PTH1R receptor (Philbrick et al. 1998; Richman 2019; Takahashi et al. 2019). It is clear that in the gecko there is no eruption pathway during the normal course of tooth shedding. Instead, we have shown here that the functional teeth are invaded by odontoclasts. This timed, tooth resorption in geckos may recapitulate the features of an eruption pathway in the mammal. The odontoclasts of geckos do express the same markers as osteoclasts (RANKL, CTSK) in humans (Iglesias-Linares and Hartsfield 2017; Wang and McCauley 2011). These molecular profiles of odontoclasts involved in physiological tooth resorption are an extension of the TRAP staining been reported in resorbing human deciduous molars (Sahara et al. 1996; Takada et al. 2004).

An unexpected finding was the discovery of chemotaxis genes in the functional teeth. We were not able to detect the presence of *SEMA3A* and *SEMA3E* in the single cell RNAseq. The

expression of the SEMA3A gene is of particular interest and may play a dual role in recruitment of odontoclasts and axon guidance. Thus far the data in mouse studies suggests that SEMA3A is expressed in the osteoclasts that are creating the eruption pathway (Yu et al. 2019). In addition, the SEMA3A receptors Neuropilin 1 and Plexin A1 are also expressed during tooth eruption. Other studies have localized SEMA3A protein in osteoblasts and osteocytes (Xu 2014). We did not find *SEMA3A* transcripts in the bone but instead found transcripts between the functional teeth. Further in vivo experiments are needed to test the role of SEMA3A, CTSK and RANKL in directing tooth resorption in the gecko.

In conclusion the comparison of transcriptomes in a polyphyodont reptile to those of the mouse have already revealed stark differences. Our studies suggest that there has been independent (convergent) evolution of the trait of tooth eruption in lizards and snakes. Moreover, the second generation teeth likely do communicate with the functional teeth as shown by our work. We removed second generation teeth and followed the eruption process for many months. The functional teeth were retained longer in sites where there were no immediate successors (Brink et al. 2022). Thus instead of an eruption pathway as in the mammal, the gecko and other squamate reptiles use the enamel organ of the successional teeth to trigger tooth resorption of the functional teeth, thus creating an eruption pathway. New molecules such as SEMA3A may also participate in this process. The profile of stem cells differs from the mouse incisor. Future studies on the gecko will uncover the molecular basis of convergent evolution in the dentition.

METHODS

Total RNA extraction for bulk RNA sequencing or qRT-PCR

We removed functional and developing, unerupted teeth and these were pooled into three biological replicates for bulk RNA sequencing (Fig. 1A). There were 3 functional or 3 developing teeth pooled for each biological replicate. For the qRT-PCR, independent biological replicates were collected and each contained 10-12 teeth. All teeth were snap frozen in liquid nitrogen. Each sample was disrupted using beads (Buffer RLT from Qiagen microRNA kit, Omni bead Ruptor 96, Lysing matrix E) followed by a Qiagen Shredder column (ID:79656). Total RNA was extracted using a Qiagen RNeasy micro kit (ID: 74004). RNA quality was determined with Agilent Bioanalyzer 2100. Samples with an RNA Integrity (RIN) greater than 7 were sequenced using Illumina Nextseq 2000 or used for qRT-PCR (Table 1).

Bulk RNA sequencing and data analysis

Qualifying samples were prepped following the standard protocol for the NEBnext Ultra ii Stranded mRNA (New England Biolabs) at Biomedical research Center sequencing Core at University of British Columbia. Sequencing was performed on the Illumina NextSeq2000 with Paired End 59bp × 59bp reads. Sequencing data was demultiplexed using Illumina's bcl2fastq2 and approximately 20 million read pairs were obtained for each sample. The bulk RNA-seq data was deposited into the National Center for Biotechnology Information Gene Expression Omnibus database (Accession GSE220653).

As previously described in Vuilleumier *et al* ((Vuilleumier et al. 2019)), multiple differential expression analysis pipelines were applied and the results combined. In the current study the pipelines primarily used the draft reference genome and transcriptome from Xiong *et al* (Xiong et al. 2016) and http://gigadb.org/dataset/100246). The important gene *CTSK* was however missing from the published annotations so we therefore called genes *de novo* with the code BRAKER ;(Barnett et al. 2011; Bruna et al. 2021; Buchfink et al. 2015; Hoff et al. 2016; Hoff et al. 2019; Li et al. 2009; Lomsadze et al. 2014; Stanke et al. 2008; Stanke et al. 2006) and https://github.com/Gaius-Augustus/BRAKER) using our RNA-seq read alignments as hints. We then extracted the *CTSK* gene structure and associated transcripts from those results and added the information to the reference genome/transcriptome before doing the differential expression analysis (Table S2). Only genes achieving a false discovery rate of 0.05 in at least half of the ten RNA-seq pipelines applied were considered as significantly differentially expressed. Volcano plots for some of the individual analysis pipelines were created using the R package Enhance Volcano plot (https://github.com/kevinblighe/EnhancedVolcano).

Several genes annotated as “unknown” in the published genome were searched using blastx against the nucleotide collection (nr/nt) (Camacho et al. 2009; Sayers et al. 2022) in order to assign more meaningful gene names. The gene names were changed to their respective human orthologue to improve the quality of post-hoc analyses. To determine gene ontology of the main biological processes in the two types of teeth, the list of differentially expressed genes was entered into the Panther Classification system (Pantherdb.org; Table S4).

qRT-PCR validation of bulk RNA-seq

Genes were selected for validation with qRT-PCR with a Log_2 fold change of at least 0.9, a false discovery rate lower than 0.05 and/or biological relevance for tooth development and osteoclast differentiation and function. In our experience, genes with base Mean normalized counts in DESeq2 greater than 200 in each of the 3 biological replicates used for sequencing gave measurable differences in signal in the qRT-PCR experiments. In our experience genes with lower counts were not always detectable. Ten nanograms of total RNA from each independent biological replicate was amplified for 2h with the Qiagen QuantiTect whole transcriptome amplification kit (Table 1). Aliquots were taken before inactivating Repli-g Midi DNA polymerase and used to quantify double stranded cDNA with Quant-iT™ PicoGreen™ kit (Thermo-Fisher). Sybr green-based quantitative qRT-PCR was conducted using a BioRad kit (#1725271; SsoAdvanced Universal SYBR-Green supermix). Primers were designed based on the gecko genome and transcriptome sequence (Table S5). Quantitative-PCR cycling conditions were: 95°C for 10min, 40X (95°C for 5s, 60°C for 20s). Gene expression levels were calculated using ΔCT method with normalization against 18s ribosomal (Applied Biosystems #4318839). All qRT-PCR reactions were performed in triplicate for each sample, four biological replicates were analyzed for each type of tooth (Table 1). T-tests of ΔCT values were computed to determine statistically significant differences in expression between functional and developing teeth. ΔΔCT were computed by subtracting the respective ΔCT value to the average ΔCT of functional teeth sample for each gene. The fold change ΔΔCT was plotted (Fig. 2B, Fig. S2B,C).

Single Cell RNAseq

In order to identify cell subpopulations in the odontogenic regions of the jaws, we dissected tissues enclosing oral mucosa, dental lamina, dental mesenchyme, immature cap and bud stage teeth and bell stage, mineralizing teeth (Fig. 1B). Tissues were dissected and placed in cold 1X HANKS solution without Calcium and Magnesium and 10% fetal bovine serum (FBS, Gibco). The tissues were chopped into small segments. Then, they were placed in the dissection media with collagenase D/ Dispase II (SIGMA cat no. 11231857001/SIGMA cat no. D4693) for 37°C for 4-5 hours in an orbital shaker. Alternatively, the tissue from the second animal was dissociated with a cold temperature enzyme protease from *Bacillus lichenoformis* (cat no. Sigma p5380) for 6 hours at 4°C. Once the cells were dissociated, cells were spun down and counted.

They were transferred into FACS buffer (2 mM EDTA, 2% FBS, 1X PBS) and resuspended in 2 ml final volume. Cells were passed through a 70 µm cell filter to remove clumps. Live versus dead cells were distinguished with propidium iodide exclusion (1:5000 in FACS buffer). Cells were sorted in DMEM + 5% FBS media in a Beckman Coulter Cytoflex LX Analyzer . Cells were concentrated to 50,000 cell/ml. The cell suspension was loaded on the 10x genomics single cell controller for capture in droplet emulsion. Libraries were prepped using the Chromium Single Cell 3' Reagent v3 Chemistry kit and the standard protocol was followed for all steps. Libraries were then sequenced on an Illumina Nextseq500. 10x genomics Cell Ranger 2.0 was used to perform Demultiplexing, Alignment, Counting, Clustering, and Differential expression. The scRNA-seq raw and processed data were deposited to the National Center for Biotechnology Information Gene Expression Omnibus database (GEO; https://www.ncbi.nlm.nih.gov/geo/; accession number GSE221110). Cellranger exports were further analyzed using Seurat package 4.0.4. A differentially expressed gene list for each cluster was computed using the Findmarkers function (Table S2). Note that the mitochondrial genes in the gecko are not annotated so we did not filter on high levels of mitochondrial DNA in the quality control steps.

Immunofluorescence and TRAP staining

In order to identify odontoclasts, tartrate acid resistant phosphatase (TRAP) staining was carried out on paraffin sections of gecko tooth families. Slides were placed in pre-warmed TRAP solution (0.92 % Sodium Acetate Anhydrous, 1.14%, Tartaric Acid, 0.01% Napthol AS-MX Phosphate and 0.06% Fast Red Violet LB Salt; Sigma Aldrich) and incubated at 37°C for 60 mins. Slides were rinsed in distilled water, counterstained with 0.02% Fast green for 1 minute and then coverslipped.

Immunofluorescence staining was carried out on paraformaldehyde fixed tissues embedded in paraffin (Brink et al. 2021). The primaries antibodies were: anti-Cx43 (Sigma-Aldrich, C6219, 1:1000); anti-RANKL (Abcam, ab65024, 1:200); anti-CTSK (Abcam, ab37259, 1:200); anti PITX2 (R&D systems, AF7388, 1:500). Antibodies to Cx43, RANKL and CTSK were diluted in 10% goat serum, 1XPBS, and 0.1% Tween-20. PITX2 was diluted in 5% bovine serum, 0.1% Tween-20 in Tris buffered salt solution. The secondary antibodies were diluted to 1:250 (Goat anti-rabbit IgG Cy5; Invitrogen A10523; goat anti-mouse IgG AlexaFluor 488, Invitrogen A11029; goat anti-rabbit IgG AlexaFluor 488, Invitrogen A11034). Nuclei were

stained with Hoechst 33258 (Sigma, 10 mg/ml; 30 min). Slides were scanned in the fluorescence mode using a 3DHISTECH Slide scanner and a 20X objective (3DHistech.com, Hungary).

RNAscope in situ hybridization

We selected genes for validation with RNAscope from the bulk RNAseq data based primarily on biological relevance, low FDR and Log_2 fold change of at least 0.9 (functional or developing tooth samples, *SEMA3A*, *SEMA3E*, *PTHLH*). Flanking 5' and 3' UTRs plus coding sequences for each of the genes were extracted from the gecko genome in our lab. In order to find the UTRs, we used BED tools to extract the coding sequences and UTRs. We validated the sequences with the IGV browser downloaded from the Broad Institute. We next confirmed that there was little homology to other related family members using nr Blast against *Gekko japonicus*. In the case of *COL1A1*, areas of very highly conserved sequence between *COL1A1* and *COL1A2* were avoided. These trimmed sequences were provided to the company ACDBio who then designed custom DNA probes. The probes used are: Emac-SEMA3A-C1 (ref 1099931-C1), Emac-*SEMA3E*-C1 (ref 1099911), Emac-*PTHLH*-C1 (ref1208601-C1), *COL1A1*, Emac-*COL1A1-C1* (ref 1214171-C1). The following ZZ pairs were used: Emac-SEMA3A,18ZZ probe targeting 47-912 of the provided sequence; 20ZZ probe named Emac-SEMA3E targeting 344-1312 of the provided sequence; 10ZZ probe named Emac-PTHLH targeting 16-525 of the provided sequence; 20ZZ probe named Emac-COL1A1 targeting 251-1133 of the provided sequence. *COL1A1* was used as a positive control for the in situ hybridization conditions. The RNAscope 2.5 HD detection red kit was used according to manufacturer indications with the following modifications: Amplification step 5 was carried out for 50 minutes for all probes except for *PTHLH* which was carried for 90 minutes. Slides were coverslipped and scanned with a 3DHISTECH Slide scanner (3DHistech.com, Hungary) using a 20X objective with brightfield illumination.

Funding

The experimental work was funded by NSERC grant RGPIN-2016-05477 and NIH grant 5R21DE026839-02 to JMR.

Conflict of Interest statement:

Authors declare that the research was conducted in the absence of any commercial or financial relationships that could be construed as a potential conflict of interest.

Acknowledgements

The authors would like to thank the Biomedical Research Sequencing core at UBC (Tara Stach and Ryan Vander Werff), Preety Panwar and Dieter Bromme for providing initial reagents to stain odontoclasts and Mark Sgro for help with blasting the gecko sequences.

References

Adam M., Potter A. S., Potter S. S. (2017). Psychrophilic proteases dramatically reduce single-cell rna-seq artifacts: A molecular atlas of kidney development. *Development*. **144**:3625-3632.

Barnett D. W., Garrison E. K., Quinlan A. R., Stromberg M. P., Marth G. T. (2011). Bamtools: A c++ api and toolkit for analyzing and managing bam files. *Bioinformatics*. **27**:1691-1692.

Bartlett J. D., Simmer J. P. (2015). New perspectives on amelotin and amelogenesis. *J Dent Res*. **94**:642-644.

Bertin T. J. C., Thivichon-Prince B., LeBlanc A. R. H., Caldwell M. W., Viriot L. (2018). Current perspectives on tooth implantation, attachment, and replacement in amniota. *Front Physiol*. **9**:1630.

Brink K. S., Cytrynbaum E., Grieco T. M., Henriquez J. I., Zhitnitsky A., Richman J. M. (2022). Evolutionarily conserved waves of tooth replacement in the gecko are dependent on local signaling. First two authors contributed equally. *BioRxiv.org*. **BIORXIV/2022/513312**.

Brink K. S., Henriquez J. I., Grieco T. M., Martin Del Campo J. R., Fu K., Richman J. M. (2021). Tooth removal in the leopard gecko and the de novo formation of replacement teeth. *Front Physiol*. **12**:576816.

Brink K. S., Wu P., Chuong C. M., Richman J. M. (2020). The effects of premature tooth extraction and damage on replacement timing in the green iguana. *Integr Comp Biol*. **60**:581-593.

Bruna T., Hoff K. J., Lomsadze A., Stanke M., Borodovsky M. (2021). Braker2: Automatic eukaryotic genome annotation with genemark-ep+ and augustus supported by a protein database. *NAR Genom Bioinform*. **3**:lqaa108.

Buchfink B., Xie C., Huson D. H. (2015). Fast and sensitive protein alignment using diamond. *Nat Methods*. **12**:59-60.

Buchtová M., Boughner J. C., Fu K., Diewert V. M., Richman J. M. (2007). Embryonic development of python sebae - ii: Craniofacial microscopic anatomy, cell proliferation and apoptosis. *Zoology (Jena)*. **110**:231-251.

Buchtova M., Zahradnicek O., Balkova S., Tucker A. S. (2013). Odontogenesis in the veiled chameleon (chamaeleo calyptratus). *Arch Oral Biol*. **58**:118-133.

Cahill D. R., Marks S. C., Jr. (1980). Tooth eruption: Evidence for the central role of the dental follicle. *J Oral Pathol*. **9**:189-200.

Camacho C., Coulouris G., Avagyan V., Ma N., Papadopoulos J., Bealer K., Madden T. L. (2009). Blast+: Architecture and applications. *BMC Bioinformatics*. **10**:421.

Cheng Y., Lotan R. (1998). Molecular cloning and characterization of a novel retinoic acid-inducible gene that encodes a putative g protein-coupled receptor. *J Biol Chem*. **273**:35008-35015.

Chiba Y., Saito K., Martin D., Boger E. T., Rhodes C., Yoshizaki K., Nakamura T., Yamada A., Morell R. J., Yamada Y. et al. (2020). Single-cell rna-sequencing from mouse incisor reveals dental epithelial cell-type specific genes. *Front Cell Dev Biol*. **8**:841.

Choi Y. S., Chakrabarti R., Escamilla-Hernandez R., Sinha S. (2009). Elf5 conditional knockout mice reveal its role as a master regulator in mammary alveolar development: Failure of stat5 activation and functional differentiation in the absence of elf5. *Dev Biol*. **329**:227-241.

Choi Y. S., Cheng J., Segre J., Sinha S. (2008). Generation and analysis of elf5-lacz mouse: Unique and dynamic expression of elf5 (ese-2) in the inner root sheath of cycling hair follicles. *Histochem Cell Biol*. **129**:85-94.

Cooper J. S. (1966). Tooth replacement in the slow worm (anguis fragilis). *Journal of Zoology*. **150**:235–248.

Domingues M. G., Jaeger M. M., Araujo V. C., Araujo N. S. (2000). Expression of cytokeratins in human enamel organ. *Eur J Oral Sci*. **108**:43-47.

Dong X., Shen B., Ruan N., Guan Z., Zhang Y., Chen Y., Hu X. (2014). Expression patterns of genes critical for bmp signaling pathway in developing human primary tooth germs. *Histochem Cell Biol*. **142**:657-665.

Edmund A. G. (1962). Sequence and rate of tooth replacement in the crocodilia. *Contributions of the Life Sciences Division, Royal Ontario Museum Toronto*. **56**:7–42.

Emanuele M. J., Ciccia A., Elia A. E., Elledge S. J. (2011). Proliferating cell nuclear antigen (pcna)-associated kiaa0101/paf15 protein is a cell cycle-regulated anaphase-promoting complex/cyclosome substrate. *Proc Natl Acad Sci U S A*. **108**:9845-9850.

Fraser G. J., Bloomquist R. F., Streelman J. T. (2013). Common developmental pathways link tooth shape to regeneration. *Dev Biol*. **377**:399-414.

Fu X., Xu J., Chaturvedi P., Liu H., Jiang R., Lan Y. (2017). Identification of osr2 transcriptional target genes in palate development. *J Dent Res*. **96**:1451-1458.

Fuenzalida M., Illanes J., Lemus R., Guerrero A., Oyarzun A., Acuna O., Lemus D. (1999). Microscopic and histochemical study of odontoclasts in physiologic resorption of teeth of the polyphyodont lizard, liolaemus gravenhorsti. *J Morphol*. **242**:295-309.

Gautier J., Norbury C., Lohka M., Nurse P., Maller J. (1988). Purified maturation-promoting factor contains the product of a xenopus homolog of the fission yeast cell cycle control gene cdc2+. *Cell*. **54**:433-439.

Grieco T. M., Richman J. M. (2018). Coordination of bilateral tooth replacement in the juvenile gecko is continuous with in ovo patterning. *Evol Dev*. **20**:51-64.

Grigoriou M., Tucker A. S., Sharpe P. T., Pachnis V. (1998). Expression and regulation of lhx6 and lhx7, a novel subfamily of lim homeodomain encoding genes, suggests a role in mammalian head development. *Development*. **125**:2063-2074.

Handrigan G. R., Leung K. J., Richman J. M. (2010). Identification of putative dental epithelial stem cells in a lizard with life-long tooth replacement. *Development*. **137**:3545-3549.

Handrigan G. R., Richman J. M. (2010). Autocrine and paracrine shh signaling are necessary for tooth morphogenesis, but not tooth replacement in snakes and lizards (squamata). *Dev Biol*. **337**:171-186.

Handrigan G. R., Richman J. M. (2011). Unicuspid and bicuspid tooth crown formation in squamates. *J Exp Zool B Mol Dev Evol*. **316**:598-608.

Harada H., Kettunen P., Jung H. S., Mustonen T., Wang Y. A., Thesleff I. (1999). Localization of putative stem cells in dental epithelium and their association with notch and fgf signaling. *J Cell Biol*. **147**:105-120.

Higashihori N., Lehnertz B., Sampaio A., Underhill T. M., Rossi F., Richman J. M. (2017). Methyltransferase g9a regulates osteogenesis via twist gene repression. *J Dent Res*. **96**:1136-1144.

Hoff K. J., Lange S., Lomsadze A., Borodovsky M., Stanke M. (2016). Braker1: Unsupervised rna-seq-based genome annotation with genemark-et and augustus. *Bioinformatics*. **32**:767-769.

Hoff K. J., Lomsadze A., Borodovsky M., Stanke M. (2019). Whole-genome annotation with braker. *Methods Mol Biol*. **1962**:65-95.

Hu J. C., Simmer J. P. (2007). Developmental biology and genetics of dental malformations. *Orthod Craniofac Res*. **10**:45-52.

Iglesias-Linares A., Hartsfield J. K., Jr. (2017). Cellular and molecular pathways leading to external root resorption. *J Dent Res*. **96**:145-152.

Jackson M. F., Scatena M., Giachelli C. M. (2017). Osteoclast precursors do not express cd68: Results from cd68 promoter-driven rank transgenic mice. *FEBS Lett*. **591**:728-736.

Jarvinen E., Tummers M., Thesleff I. (2009). The role of the dental lamina in mammalian tooth replacement. *J Exp Zoolog B Mol Dev Evol*.

Järvinen E., Välimäki K., Pummila M., Thesleff I., Jernvall J. (2008). The taming of the shrew milk teeth. *Evol Dev*. **10**:477-486.

Jing J., Feng J., Yuan Y., Guo T., Lei J., Pei F., Ho T. V., Chai Y. (2022). Spatiotemporal single-cell regulatory atlas reveals neural crest lineage diversification and cellular function during tooth morphogenesis. *Nat Commun*. **13**:4803.

Jones C. A., London N. R., Chen H., Park K. W., Sauvaget D., Stockton R. A., Wythe J. D., Suh W., Larrieu-Lahargue F., Mukouyama Y. S. et al. (2008). Robo4 stabilizes the vascular network by inhibiting pathologic angiogenesis and endothelial hyperpermeability. *Nat Med*. **14**:448-453.

Juuri E., Balic A. (2017). The biology underlying abnormalities of tooth number in humans. *J Dent Res*. **96**:1248-1256.

Kim E. J., Jung S. Y., Wu Z., Zhang S., Jung H. S. (2020). Sox2 maintains epithelial cell proliferation in the successional dental lamina. *Cell Prolif*. **53**:e12729.

Kim J., Oh W. J., Gaiano N., Yoshida Y., Gu C. (2011). Semaphorin 3e-plexin-d1 signaling regulates vegf function in developmental angiogenesis via a feedback mechanism. *Genes Dev*. **25**:1399-1411.

Kline L. W., Cullum D. (1984). A long-term study of the tooth replacement phenomenon in the young green iguana, iguana-iguana. *Journal of Herpetology*. **18**:176-185.

Krivanek J., Soldatov R. A., Kastriti M. E., Chontorotzea T., Herdina A. N., Petersen J., Szarowska B., Landova M., Matejova V. K., Holla L. I. et al. (2020). Dental cell type atlas reveals stem and differentiated cell types in mouse and human teeth. *Nat Commun*. **11**:4816.

Laurikkala J., Mikkola M., Mustonen T., Aberg T., Koppinen P., Pispa J., Nieminen P., Galceran J., Grosschedl R., Thesleff I. (2001). Tnf signaling via the ligand-receptor pair ectodysplasin and edar controls the function of epithelial signaling centers and is regulated by wnt and activin during tooth organogenesis. *Dev Biol*. **229**:443-455.

LeBlanc A. R. H., Lamoureux D. O., Caldwell M. W. (2017). Mosasaurs and snakes have a periodontal ligament: Timing and extent of calcification, not tissue complexity, determines tooth attachment mode in reptiles. *J Anat*. **231**:869-885.

LeBlanc A. R. H., Paparella I., Lamoureux D. O., Doschak M. R., Caldwell M. W. (2021). Tooth attachment and pleurodont implantation in lizards: Histology, development, and evolution. *J Anat*. **238**:1156-1178.

Lee S., Bush S. J., Thorne S., Mawson N., Farquharson C., Bergkvist G. T. (2020). Transcriptomic profiling of feline teeth highlights the role of matrix metalloproteinase 9 (mmp9) in tooth resorption. *Sci Rep*. **10**:18958.

Li H., Handsaker B., Wysoker A., Fennell T., Ruan J., Homer N., Marth G., Abecasis G., Durbin R., Genome Project Data Processing S. (2009). The sequence alignment/map format and samtools. *Bioinformatics*. **25**:2078-2079.

Lomsadze A., Burns P. D., Borodovsky M. (2014). Integration of mapped rna-seq reads into automatic training of eukaryotic gene finding algorithm. *Nucleic Acids Res*. **42**:e119.

Luukko K., Kettunen P. (2016). Integration of tooth morphogenesis and innervation by local tissue interactions, signaling networks, and semaphorin 3a. *Cell Adh Migr*. **10**:618-626.

Mendoza-Londono R., Fahiminiya S., Majewski J., Care4Rare Canada C., Tetreault M., Nadaf J., Kannu P., Sochett E., Howard A., Stimec J. et al. (2015). Recessive osteogenesis imperfecta caused by missense mutations in sparc. *Am J Hum Genet*. **96**:979-985.

Meng T., Huang Y., Wang S., Zhang H., Dechow P. C., Wang X., Qin C., Shi B., D'Souza R. N., Lu Y. (2015). Twist1 is essential for tooth morphogenesis and odontoblast differentiation. *J Biol Chem*. **290**:29593-29602.

Moe K., Shrestha A., Kvinnsland I. H., Luukko K., Kettunen P. (2012a). Developmentally regulated expression of sema3a chemorepellant in the developing mouse incisor. *Acta Odontol Scand*. **70**:184-189.

Moe K., Sijaona A., Shrestha A., Kettunen P., Taniguchi M., Luukko K. (2012b). Semaphorin 3a controls timing and patterning of the dental pulp innervation. *Differentiation*. **84**:371-379.

Moradian-Oldak J., George A. (2021). Biomineralization of enamel and dentin mediated by matrix proteins. *J Dent Res*. **100**:1020-1029.

Morita M., Yoshida S., Iwasaki R., Yasui T., Sato Y., Kobayashi T., Watanabe R., Oike T., Miyamoto K., Takami M. et al. (2016). Smad4 is required to inhibit osteoclastogenesis and maintain bone mass. *Sci Rep*. **6**:35221.

Nagata M., Chu A. K. Y., Ono N., Welch J. D., Ono W. (2021). Single-cell transcriptomic analysis reveals developmental relationships and specific markers of mouse periodontium cellular subsets. *Front Dent Med*. **2**.

Nagata M., Ono N., Ono W. (2020). Mesenchymal progenitor regulation of tooth eruption: A view from pthrp. *J Dent Res*. **99**:133-142.

Nakchbandi I. A., Weir E. E., Insogna K. L., Philbrick W. M., Broadus A. E. (2000). Parathyroid hormone-related protein induces spontaneous osteoclast formation via a paracrine cascade. *Proc Natl Acad Sci U S A*. **97**:7296-7300.

Neuhaus S. J., Byers M. R. (2007). Endothelin receptors and endothelin-1 in developing rat teeth. *Arch Oral Biol*. **52**:655-662.

Ono W., Sakagami N., Nishimori S., Ono N., Kronenberg H. M. (2016). Parathyroid hormone receptor signalling in osterix-expressing mesenchymal progenitors is essential for tooth root formation. *Nat Commun*. **7**:11277.

Ooë T. 1981. Human tooth and dental arch development. Tokyo: Ishiyaku Publishers Inc.

Pagella P., Stadlinger B., Mitsiadis T. A. (2021). Isolation of dental pulp and periodontal cells from human teeth for single-cell rna sequencing. *STAR Protoc*. **2**:100953.

Peled A., Sarig O., Samuelov L., Bertolini M., Ziv L., Weissglas-Volkov D., Eskin-Schwartz M., Adase C. A., Malchin N., Bochner R. et al. (2016). Mutations in tspear, encoding a

regulator of notch signaling, affect tooth and hair follicle morphogenesis. *PLoS Genet*. **12**:e1006369.

Philbrick W. M., Dreyer B. E., Nakchbandi I. A., Karaplis A. C. (1998). Parathyroid hormone-related protein is required for tooth eruption. *Proc Natl Acad Sci U S A*. **95**:11846-11851.

Popa E. M., Buchtova M., Tucker A. S. (2019). Revitalising the rudimentary replacement dentition in the mouse. *Development*. **146**.

Porter R. M., Lane E. B. (2003). Phenotypes, genotypes and their contribution to understanding keratin function. *Trends Genet*. **19**:278-285.

Rao S., Cronin S. J. F., Sigl V., Penninger J. M. (2018). Rankl and rank: From mammalian physiology to cancer treatment. *Trends Cell Biol*. **28**:213-223.

Richman J. M. (2019). Shedding new light on the mysteries of tooth eruption. *Proc Natl Acad Sci U S A*. **116**:353-355.

Richter L., Oberlander V., Schmidt G. (2020). Rhoa/c inhibits proliferation by inducing the synthesis of gprc5a. *Sci Rep*. **10**:12532.

Rostampour N., Appelt C. M., Abid A., Boughner J. C. (2019). Expression of new genes in vertebrate tooth development and p63 signaling. *Dev Dyn*. **248**:744-755.

Sahara N. (2001). Cellular events at the onset of physiological root resorption in rabbit deciduous teeth. *Anat Rec*. **264**:387-396.

Sahara N., Toyoki A., Ashizawa Y., Deguchi T., Suzuki K. (1996). Cytodifferentiation of the odontoclast prior to the shedding of human deciduous teeth: An ultrastructural and cytochemical study. *Anat Rec*. **244**:33-49.

Salmivirta K., Gullberg D., Hirsch E., Altruda F., Ekblom P. (1996). Integrin subunit expression associated with epithelial-mesenchymal interactions during murine tooth development. *Dev Dyn*. **205**:104-113.

Salomies L., Eymann J., Khan I., Di-Poi N. (2019). The alternative regenerative strategy of bearded dragon unveils the key processes underlying vertebrate tooth renewal. *Elife*. **8**.

Sarkar L., Sharpe P. T. (1999). Expression of wnt signalling pathway genes during tooth development. *Mech Dev*. **85**:197-200.

Sayers E. W., Bolton E. E., Brister J. R., Canese K., Chan J., Comeau D. C., Connor R., Funk K., Kelly C., Kim S. et al. (2022). Database resources of the national center for biotechnology information. *Nucleic Acids Res*. **50**:D20-D26.

Sharir A., Marangoni P., Zilionis R., Wan M., Wald T., Hu J. K., Kawaguchi K., Castillo-Azofeifa D., Epstein L., Harrington K. et al. (2019). A large pool of actively cycling progenitors orchestrates self-renewal and injury repair of an ectodermal appendage. *Nat Cell Biol*. **21**:1102-1112.

Shrestha A., Moe K., Luukko K., Taniguchi M., Kettunen P. (2014). Sema3a chemorepellant regulates the timing and patterning of dental nerves during development of incisor tooth germ. *Cell Tissue Res*. **357**:15-29.

Song E. A. C., Smalley K., Oyelakin A., Horeth E., Che M., Wrynn T., Osinski J., Romano R. A., Sinha S. (2022). Genetic study of elf5 and ehf in the mouse salivary gland. *J Dent Res*. 10.1177/00220345221130258:220345221130258.

St Hilaire C., Ziegler S. G., Markello T. C., Brusco A., Groden C., Gill F., Carlson-Donohoe H., Lederman R. J., Chen M. Y., Yang D. et al. (2011). Nt5e mutations and arterial calcifications. *N Engl J Med*. **364**:432-442.

Stanke M., Diekhans M., Baertsch R., Haussler D. (2008). Using native and syntenically mapped cdna alignments to improve de novo gene finding. *Bioinformatics*. **24**:637-644.

Stanke M., Schoffmann O., Morgenstern B., Waack S. (2006). Gene prediction in eukaryotes with a generalized hidden markov model that uses hints from external sources. *BMC Bioinformatics*. **7**:62.

Takada K., Kajiya H., Fukushima H., Okamoto F., Motokawa W., Okabe K. (2004). Calcitonin in human odontoclasts regulates root resorption activity via protein kinase a. *J Bone Miner Metab*. **22**:12-18.

Takahashi A., Nagata M., Gupta A., Matsushita Y., Yamaguchi T., Mizuhashi K., Maki K., Ruellas A. C., Cevidanes L. S., Kronenberg H. M. et al. (2019). Autocrine regulation of mesenchymal progenitor cell fates orchestrates tooth eruption. *Proc Natl Acad Sci U S A*. **116**:575-580.

Thesleff I. (2014). Current understanding of the process of tooth formation: Transfer from the laboratory to the clinic. *Aust Dent J*. **59 Suppl 1**:48-54.

Toth K., Shao Q., Lorentz R., Laird D. W. (2010). Decreased levels of cx43 gap junctions result in ameloblast dysregulation and enamel hypoplasia in gja1jrt/+ mice. *J Cell Physiol*. **223**:601-609.

Tucker A. S., Fraser G. J. (2014). Evolution and developmental diversity of tooth regeneration. *Semin Cell Dev Biol*. S1084-9521(13)00142-0 [pii]

10.1016/j.semcdb.2013.12.013.

Vaahtokari A., Aberg T., Jernvall J., Keranen S., Thesleff I. (1996). The enamel knot as a signaling center in the developing mouse tooth. *Mech Dev*. **54**:39-43.

Vonk F. J., Admiraal J. F., Jackson K., Reshef R., de Bakker M. A. G., Vanderschoot K., van den Berge I., van Atten M., Burgerhout E., Beck A. et al. (2008). Evolutionary origin and development of snake fangs. *Nature*. **454**:630-633.

Vuilleumier R., Lian T., Flibotte S., Khan Z. N., Fuchs A., Pyrowolakis G., Allan D. W. (2019). Retrograde bmp signaling activates neuronal gene expression through widespread deployment of a conserved bmp-responsive cis-regulatory activation element. *Nucleic Acids Res*. **47**:679-699.

Wang B., Li H., Liu Y., Lin X., Lin Y., Wang Y., Hu X., Zhang Y. (2014a). Expression patterns of wnt/beta-catenin signaling molecules during human tooth development. *J Mol Histol*. **45**:487-496.

Wang D., Zheng M., Lei L., Ji J., Yao Y., Qiu Y., Ma L., Lou J., Ouyang C., Zhang X. et al. (2012). Tespa1 is involved in late thymocyte development through the regulation of tcr-mediated signaling. *Nat Immunol*. **13**:560-568.

Wang F., Xiao J., Cong W., Li A., Song T., Wei F., Xu J., Zhang C., Fan Z., Wang S. (2014b). Morphology and chronology of diphyodont dentition in miniature pigs, sus scrofa. *Oral Dis*. **20**:367-379.

Wang X. P., Suomalainen M., Jorgez C. J., Matzuk M. M., Wankell M., Werner S., Thesleff I. (2004). Modulation of activin/bone morphogenetic protein signaling by follistatin is required for the morphogenesis of mouse molar teeth. *Dev Dyn*. **231**:98-108.

Wang Z., McCauley L. K. (2011). Osteoclasts and odontoclasts: Signaling pathways to development and disease. *Oral Dis*. **17**:129-142.

Wise G. E. (2009). Cellular and molecular basis of tooth eruption. *Orthod Craniofac Res*. **12**:67-73.

Wise G. E., King G. J. (2008). Mechanisms of tooth eruption and orthodontic tooth movement. *J Dent Res*. **87**:414-434.

Xiong Z., Li F., Li Q., Zhou L., Gamble T., Zheng J., Kui L., Li C., Li S., Yang H. et al. (2016). Draft genome of the leopard gecko, eublepharis macularius. *Gigascience*. **5**:47.

Xu R. (2014). Semaphorin 3a: A new player in bone remodeling. *Cell Adh Migr*. **8**:5-10.

Yamanaka A., Yasui K., Sonomura T., Iwai H., Uemura M. (2010). Development of deciduous and permanent dentitions in the upper jaw of the house shrew (suncus murinus). *Arch Oral Biol*. **55**:279-287.

Yu T., Klein O. D. (2020). Molecular and cellular mechanisms of tooth development, homeostasis and repair. *Development*. **147**.

Yu W., Li X., Eliason S., Romero-Bustillos M., Ries R. J., Cao H., Amendt B. A. (2017). Irx1 regulates dental outer enamel epithelial and lung alveolar type ii epithelial differentiation. *Dev Biol*. **429**:44-55.

Yu X., Zheng F., Du Y., Tang K., Wang W., Zhang S. (2019). Semaphorin 3a gets involved in the establishment of mouse tooth eruptive pathway. *J Mol Histol*. **50**:427-434.

Zahradnicek O., Buchtova M., Dosedelova H., Tucker A. S. (2014). The development of complex tooth shape in reptiles. *Front Physiol*. **5**:74.

Zhang Z., Lan Y., Chai Y., Jiang R. (2009). Antagonistic actions of msx1 and osr2 pattern mammalian teeth into a single row. *Science*. **323**:1232-1234.

Zhao Y., Guo Y. J., Tomac A. C., Taylor N. R., Grinberg A., Lee E. J., Huang S., Westphal H. (1999). Isolated cleft palate in mice with a targeted mutation of the lim homeobox gene lhx8. *Proc Natl Acad Sci U S A*. **96**:15002-15006.

Zhou C., Yang G., Chen M., He L., Xiang L., Ricupero C., Mao J. J., Ling J. (2015). Lhx6 and lhx8: Cell fate regulators and beyond. *FASEB J*. **29**:4083-4091.

Figure Legends

Figure 1. Diagram depicting the pipeline used to characterize the odontogenic tissues of the adult leopard gecko. Functional teeth with signs as well as developing teeth, were surgically extracted from adult animals. Total RNA was extracted from each type of samples, sequenced, and a differentially expression between functional and developing teeth was computed. Candidate transcript relevant for the process of tooth development, for clastic cells activity or recruitment and previously uncharacterized genes were validated through qRT-PCR and RNAscope (A). Oral mucosa encompassing odontogenic tissues, oral epithelium, and other associated structures were extracted from two animals. Cells were dissociated with two different enzymatic treatments. Individual alive cells were FACS sorted and submitted to single cell RNA seq to identify cell populations associated with postnatal continuous tooth replacement in these animals, cells belonging to developing teeth, cells responsible for continuous tooth shedding (B).

Figure 2. Volcano plot of transcripts sequenced in bulk RNAseq. P-value and enrichment levels for this specific plot where computed with edgeR. Dots in red are transcripts with a p-value over 0.05 and a Log_2 of the ratio between the expression level of developing and functional teeth over ± 0.9. Transcripts traditionally associated with tooth development (*LHX8*, *AMBN*, *PTHLH* and *SHH*), whose function has not been associated or we have a limited information about their role in tooth physiology (*NT5E*, *ELF3*, *SEMA3A*, *SEMA3E*, *SPARC*) and associated with odontoclast/clastic cells activity (*CSF1R* and *ACP5*) were evaluated in independent samples using qRT-PCR. Validation of significantly expressed transcript in independent samples using qRT-PCR, showing 95% confidence interval and $2^{-\Delta\Delta CT}$ values. *CSF1R* and *ACP5* were not identified as statistically significant enriched in edgeR analysis but in DESeq2 (supplementary Figure S2 and supplementary table 1). P values were calculated applying two tail t-test over the ΔCt of each sample. $P \leq 0.05$,*. $P \leq 0.01$,**. $P \leq 0.001$,***. $P \leq 0.0001$, ****.

Figure 3. Near adjacent sections stained for H and E (A), TRAP staining (B) and double immunofluorescence staining with antibodies to Cathepsin K and RANKL (C-E). A tooth family is shown in A containing a functional tooth (A') and a developing tooth (A''). TRAP staining is present in the multinuclear odontoclasts against the pulpal dentin surface (B-B')). Developing teeth do not have TRAP+ cells (B''). All TRAP+ cells had strong staining for CTSK and

RANKL (C-E'). The developing teeth had a few mononuclear TRAP+ cells (B''). The same TRAP+ cells were labeled with CTSK antibody (C'',D'') but not the RANKL antibody (E''). Scale bars: A-B, 200 µm; C-E, 100 µm; A'-E' 50 µm: A''-E'', 50 µm.

Figure 4. RNAscope staining for *SEMA3E* (A and B) and *SEMA3A* (C and D) of functional (A and C) and developing teeth (B and D) in serial sections. High magnification of the odontoblast layer of functional teeth (A', C') and regions peripheral to the dentin (A'' and C''). High magnification of developing teeth (B' and D') showing the expression of *SEMA3E* is in the most mature odontoblast of developing teeth while SEMA3A seems to be in the more immature region of the apical dental papilla. Key: bone – b, dentin – d, dental lamina – dl, oral epithelium –oe, odontoblast – od, pulp – p. Scale bars: A, B, C and D = 100 µm; A', A'', C', C'', B' and D' = 20 µm.

Figure 5. T-distributed stochastic neighbour embedding plot of single cell RNA sequence. 12 cluster were computed encompassing 6197 cells (A). Cell colored based on animal origin and enzymatic treatment used to dissociated the cells from the tissue (B). Putative epithelial cluster encircled showing the level of expression of two dental transcripts (*PITX2* and *GJA1*) (C). Putative dental mesenchymal cluster showing the levels of expression of two dental mesenchyme markers (*LHX8* and *TWIST1*) (D). Cluster 3 showing the expression of *TWIST1* and *LHX8* (E). Cluster 6 showing the expression of *GJA1* and *PITX2* (F). Number of cells with counts over 1 and indicated in righ superior corner in (E) and (F).

Figure 6. *Col1A1* was identified as statistically significantly expressed in cluster 3 in relationships to the rest of the clusters (A). RNAscope chromogenic staining of *COL1A1* in maxillary section (B). High magnification of developing teeth in B (C). Developing tooth in cap stage showing *COL1A1* staining in the dental papilla and in the surrounding mesenchyme (C'). Oral epithelium and union with dental lamina (D). Scale bar: B, 200 µm; C-D', 50 µm.

Figure 7. Violin plot showing the expression levels for three statistically significant expressed transcripts (*PITX2*, *GJA1* and *PTHLH*) in cluster 6 across all 12 clusters (A). Immunofluorescence of a tooth in histo-differentiation stage showing the expression of PITX2

across the enamel organ (B). Immunofluorescence staining of a tooth in stage of histo-differentiation showing the expression of GJA1 in the inner and outer enamel epithelium as well as in the stellate reticulum (C). High magnification of the zone of the successional lamina showing expression of GJA1 in condensing mesenchyme near the tip of the successional lamina (C'). Serial section of F stained with H&E showing epithelial cell at the tip of the successional lamina surrounded by mesenchyme (C''). H&E staining of a maxillary section across a functional teeth with sign of resorption and a developing teeth near its root (D). Chromogenic RNAscope staining for *PTHLH* of the serial section of D in the region of the inner enamel epithelium (E), region where the dental papilla encounter part of the inner enamel epithelium (F) and successional lamina starting to form a bud (G). Successional lamina – sl. Cervical loop – cl,. Stellate reticulum – sr. Outer enamel epithelium – oee. Inner enamel epithelium –iee. Odontoblast – od. Condensing mensenchyme – cm. Ameloblast – am. Scale bars: B-C, 50 µm; C'-C'', 10 µm; D, 200 µm; F, 10 µm; E and G, 20 µm.

Tables

Table 1 – Characteristics of biological replicates used for qRT-PCR

Sample number	Type of tooth	Number of teeth in the sample	RIN	Agilent concentration of original samples (ng/ul)	Concentration after amplification (ng/ul)
FT24	Functional	11	7	19	146.13
FT25	Functional	11	7.3	30	153.85
FT26	Functional	10	7.4	23	106.42
FT28	Functional	10	5.9	16	100.33
ST22	Developing	10	8.7	7	88.6
ST23	Developing	11	9.3	15	90.88
ST24	Developing	10	9	16	104.05
ST25	Developing	12	8.9	18	107.42

Figure 1

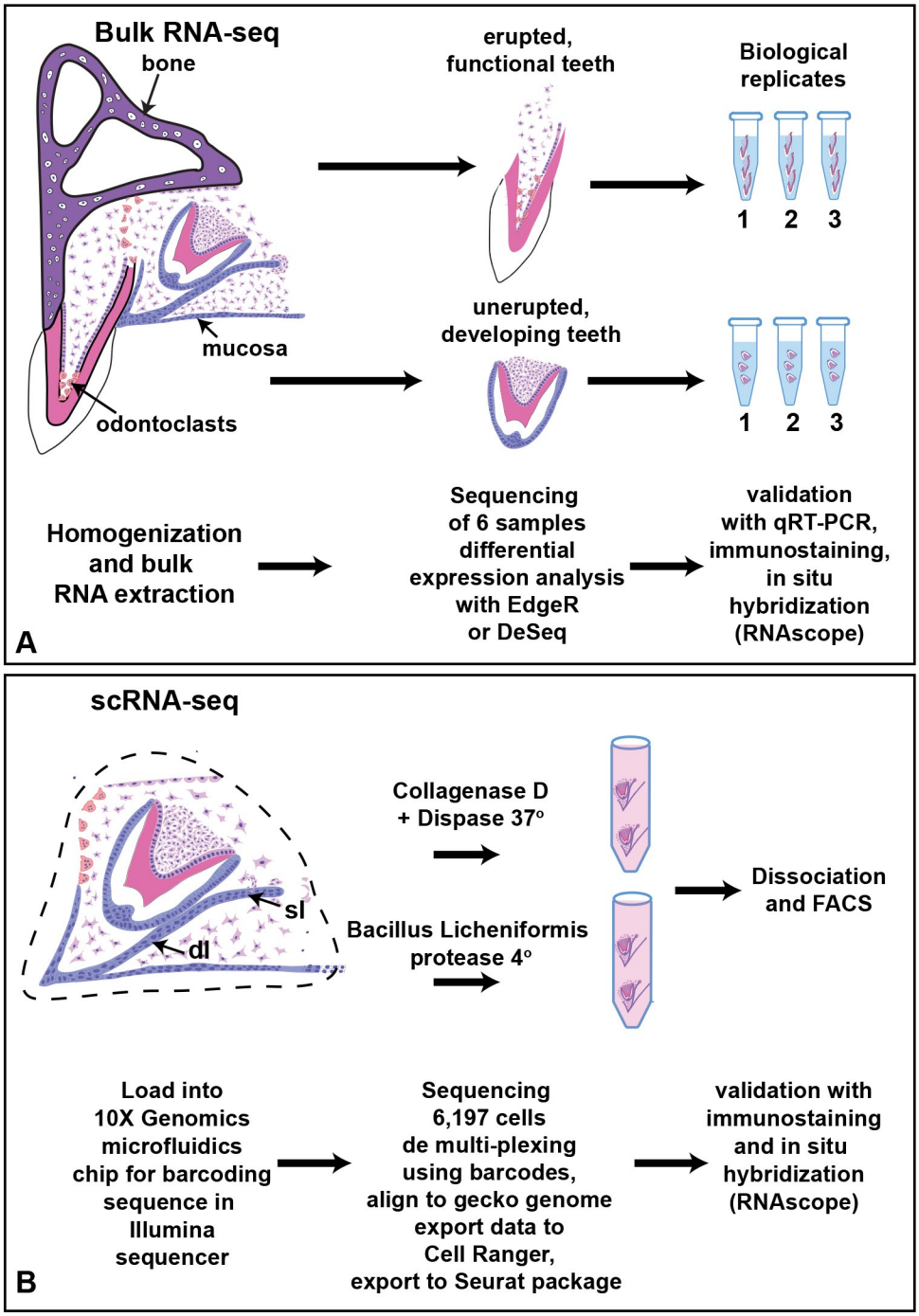
Bulk RNA-seq
bone
mucosa
odontoclasts
erupted,
functional teeth
unerupted,
developing teeth
Biological
replicates
1 2 3
1 2 3
Homogenization
and bulk
RNA extraction
Sequencing
of 6 samples
differential
expression analysis
with EdgeR
or DeSeq
validation
with qRT-PCR,
immunostaining,
in situ
hybridization
(RNAscope)
A
scRNA-seq
sl
dl
Collagenase D
+ Dispase 37°
Bacillus Licheniformis
protease 4°
Dissociation
and FACS
Load into
10X Genomics
microfluidics
chip for barcoding
sequence in
Illumina
sequencer
Sequencing
6,197 cells
de multi-plexing
using barcodes,
align to gecko genome
export data to
Cell Ranger,
export to Seurat package
validation with
immunostaining
and in situ
hybridization
(RNAscope)
B

Figure 2

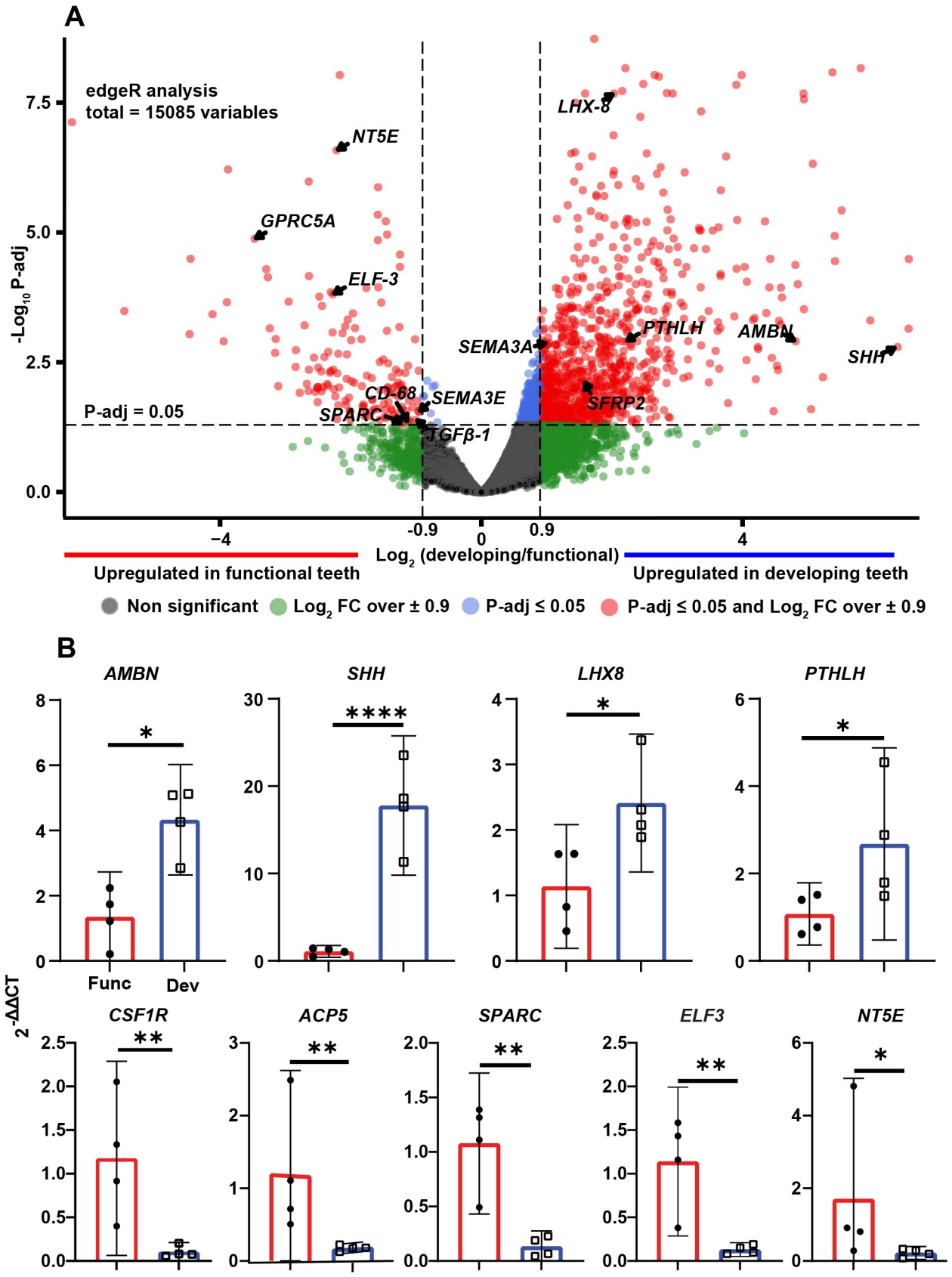
A
edgeR analysis
total = 15085 variables
NT5E
GPRC5A
ELF-3
LHX-8
SEMA3A
PTHLH
AMBN
SHH
CD-68
SEMA3E
SPARC
TGFβ-1
SFRP2
P-adj = 0.05
-Log10 P-adj
7.5
5.0
2.5
0.0
−4
-0.9
0
0.9
4
Log2 (developing/functional)
Upregulated in functional teeth
Upregulated in developing teeth
Non significant
Log2 FC over ± 0.9
P-adj ≤ 0.05
P-adj ≤ 0.05 and Log2 FC over ± 0.9
B
AMBN
SHH
LHX8
PTHLH
Func
Dev
2-ΔΔCT
CSF1R
ACP5
SPARC
ELF3
NT5E

Figure 3

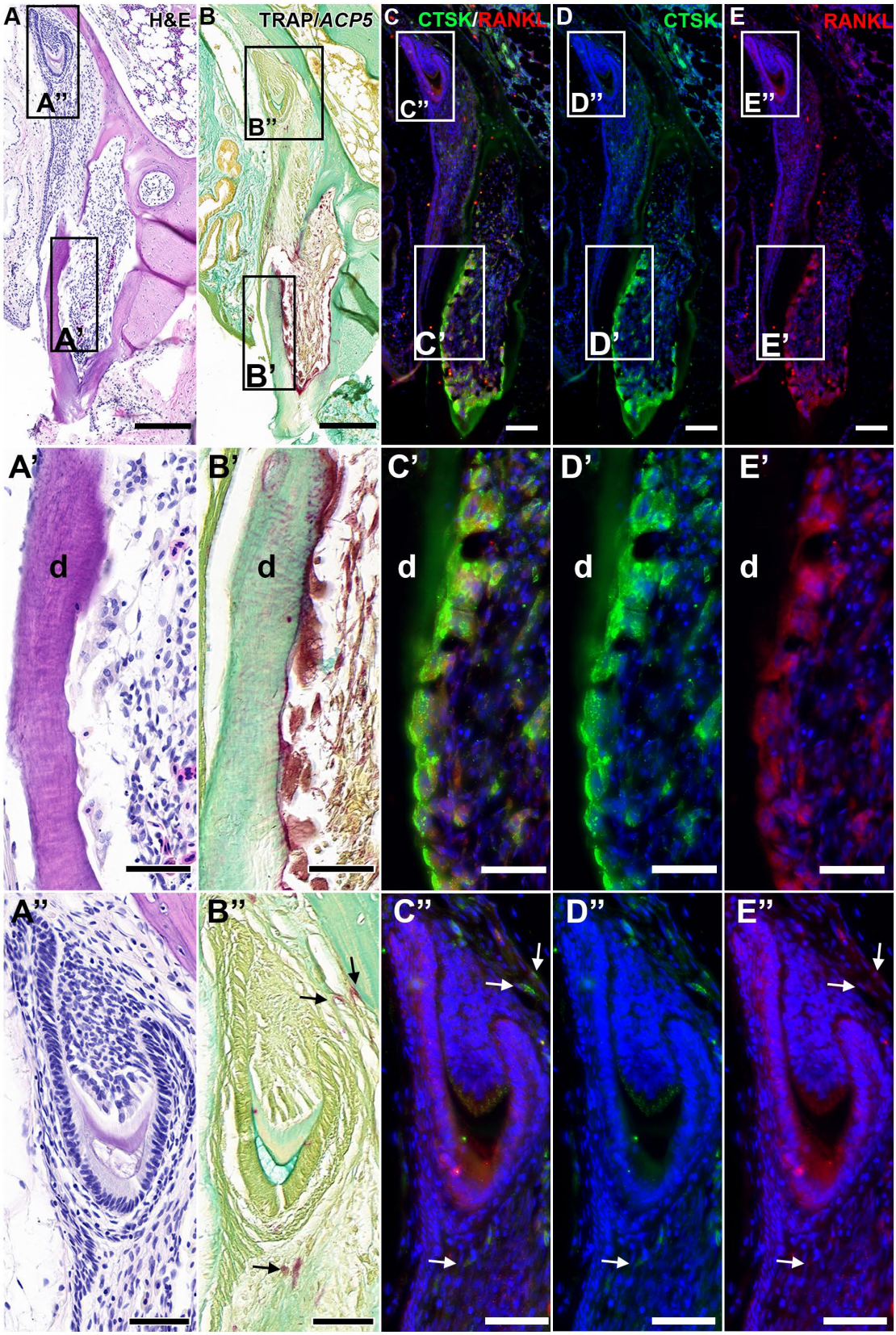

Figure 4

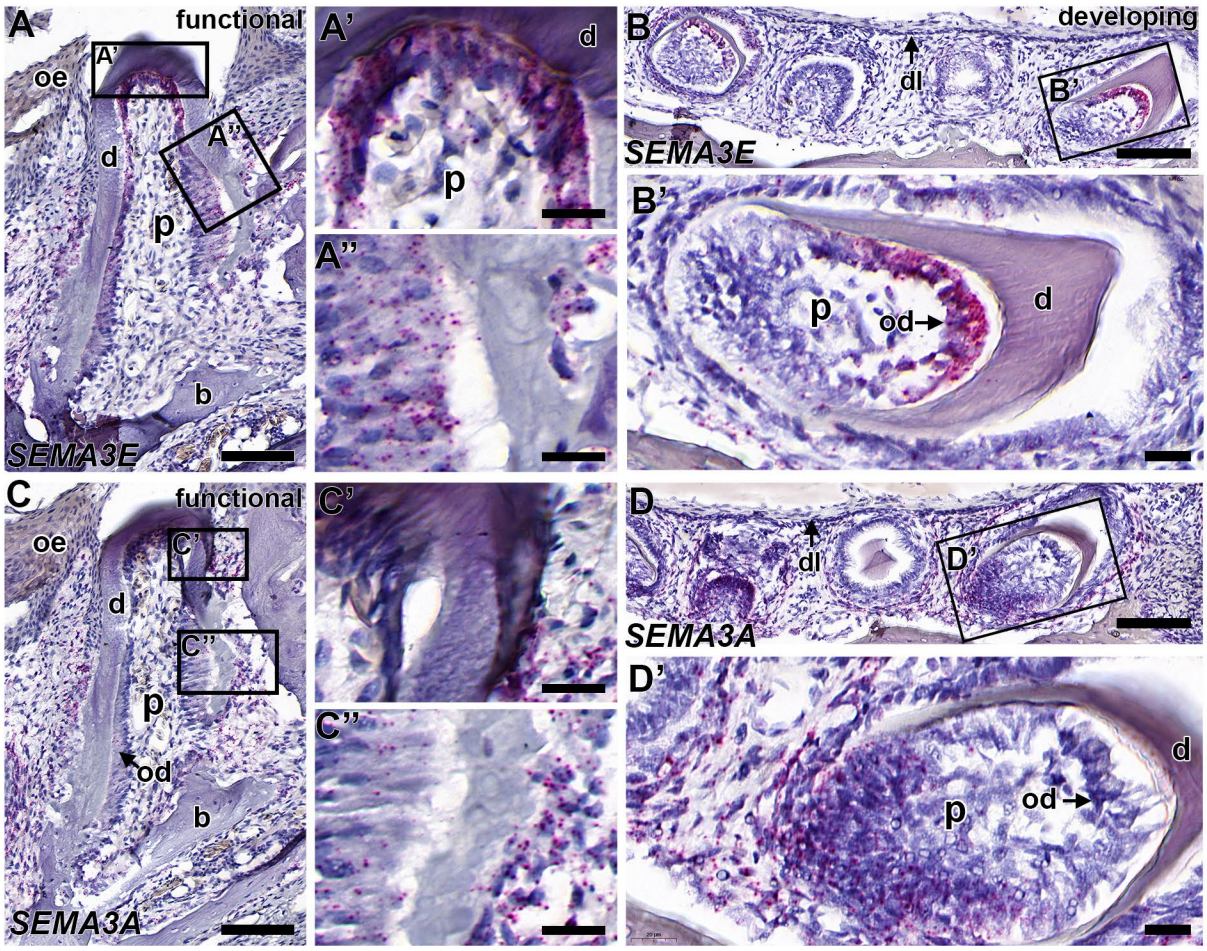
A
functional
A'
oe
A''
d
p
b
SEMA3E
A'
d
p
A''
B
developing
dl
B'
SEMA3E
B'
p
od
d
C
functional
C'
oe
d
C''
p
od
b
SEMA3A
C'
C''
D
dl
D'
SEMA3A
D'
d
p
od

Figure 5

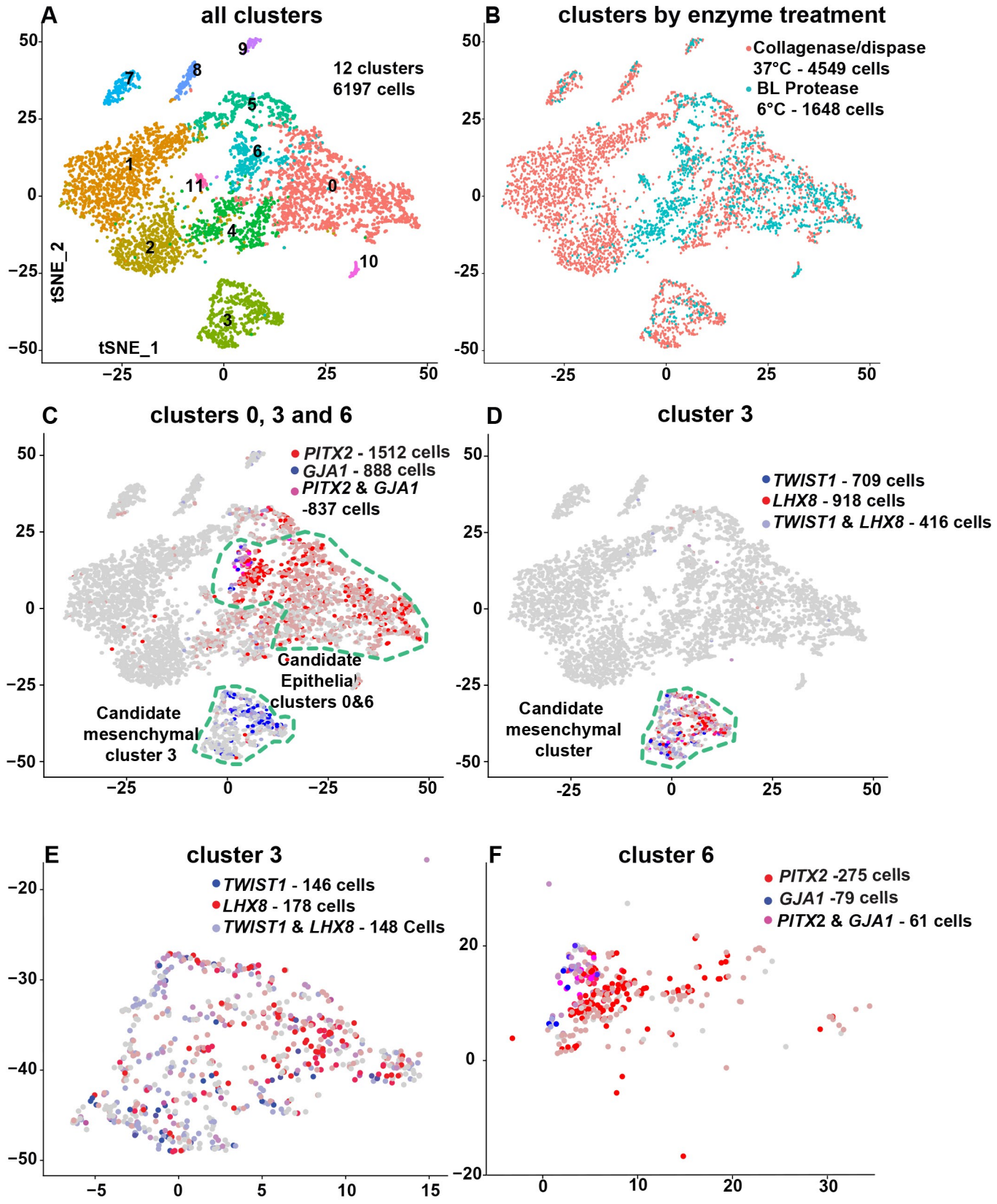
A
all clusters
12 clusters
6197 cells
tSNE_2
tSNE_1
B
clusters by enzyme treatment
Collagenase/dispase
37°C - 4549 cells
BL Protease
6°C - 1648 cells
C
clusters 0, 3 and 6
PITX2 - 1512 cells
GJA1 - 888 cells
PITX2 & GJA1
-837 cells
Candidate
Epithelial
clusters 0&6
Candidate
mesenchymal
cluster 3
D
cluster 3
TWIST1 - 709 cells
LHX8 - 918 cells
TWIST1 & LHX8 - 416 cells
Candidate
mesenchymal
cluster
E
cluster 3
TWIST1 - 146 cells
LHX8 - 178 cells
TWIST1 & LHX8 - 148 Cells
F
cluster 6
PITX2 -275 cells
GJA1 -79 cells
PITX2 & GJA1 - 61 cells

Figure 6

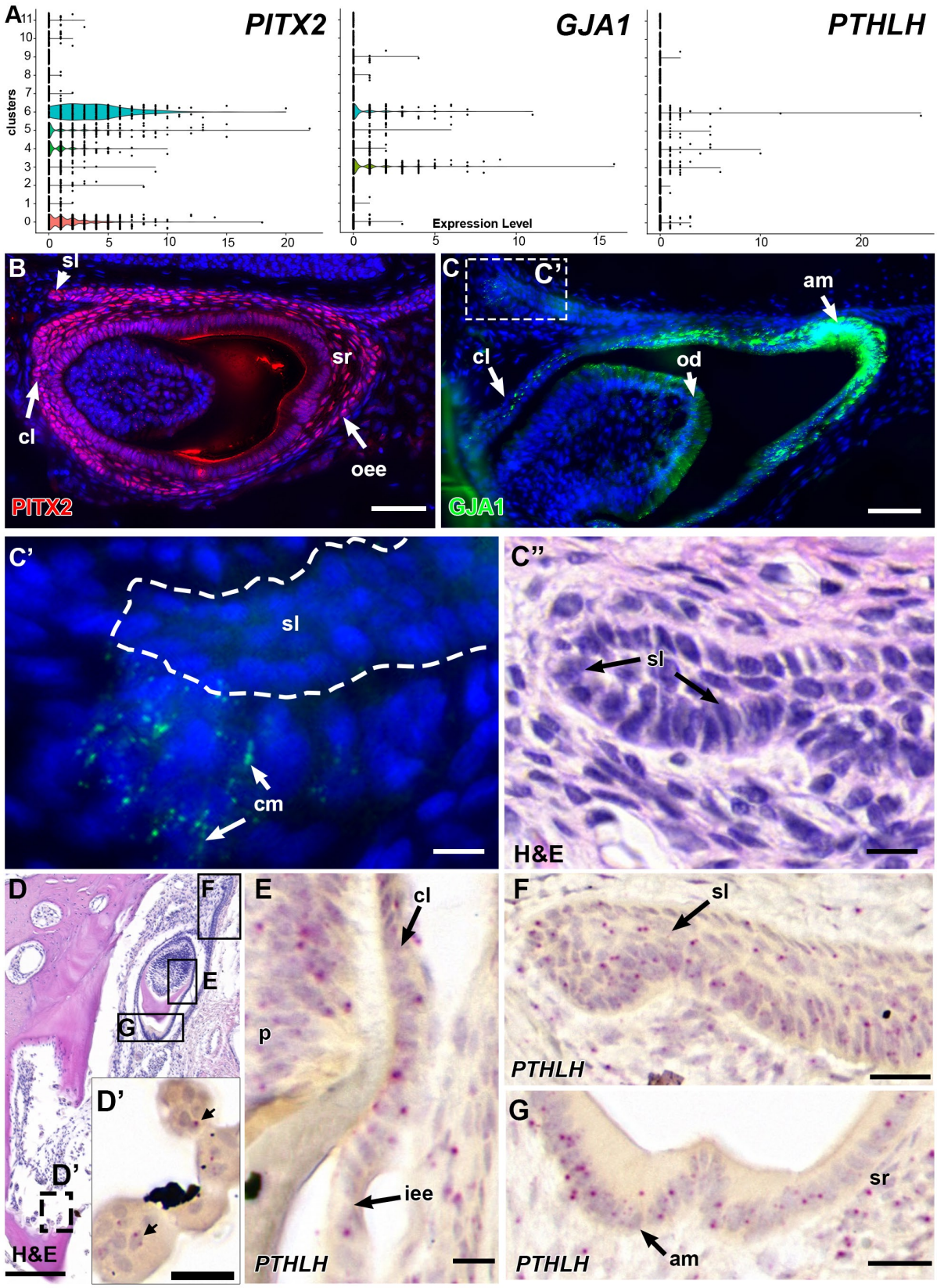
A
PITX2
GJA1
PTHLH
clusters
Expression Level
B
sl
sr
cl
oee
PITX2
C
C'
am
cl
od
GJA1
C'
sl
cm
C''
sl
H&E
D
F
E
G
D'
H&E
E
cl
p
iee
PTHLH
F
sl
PTHLH
G
sr
am
PTHLH

Figure 7

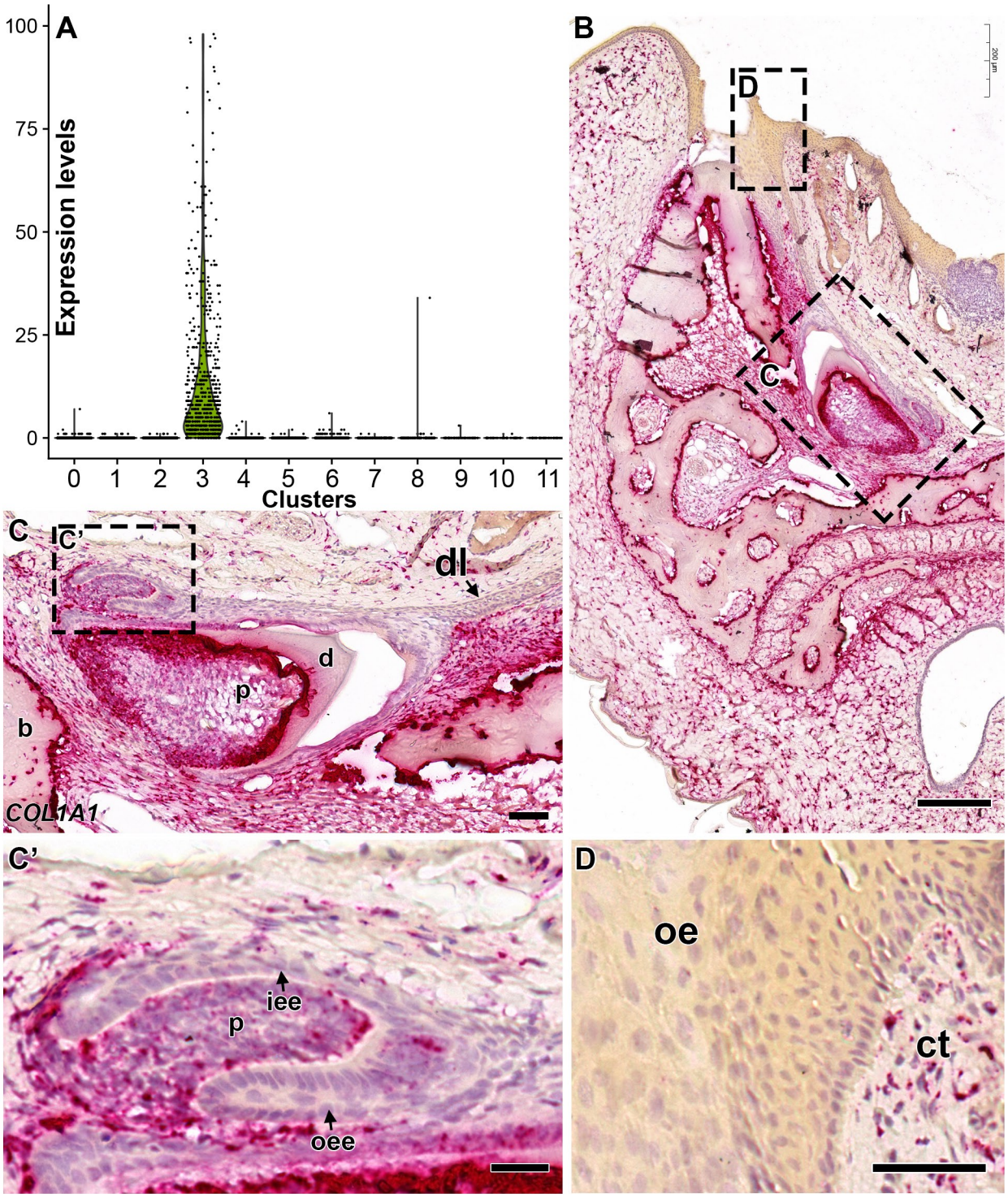
A
Expression levels
100
75
50
25
0
0 1 2 3 4 5 6 7 8 9 10 11
Clusters
B
D
C
200 µm
C
C'
dl
d
p
b
COL1A1
C'
iee
p
oee
D
oe
ct